

Wright State University

CORE Scholar

[Browse all Theses and Dissertations](#)

[Theses and Dissertations](#)

2016

Synthesis, Characterization, and Polymerization of Sulfonamide Based Bifunctional Monomers

Brady Hall
Wright State University

Follow this and additional works at: https://corescholar.libraries.wright.edu/etd_all

 Part of the [Chemistry Commons](#)

Repository Citation

Hall, Brady, "Synthesis, Characterization, and Polymerization of Sulfonamide Based Bifunctional Monomers" (2016). *Browse all Theses and Dissertations*. 1551.
https://corescholar.libraries.wright.edu/etd_all/1551

This Thesis is brought to you for free and open access by the Theses and Dissertations at CORE Scholar. It has been accepted for inclusion in Browse all Theses and Dissertations by an authorized administrator of CORE Scholar. For more information, please contact library-corescholar@wright.edu.

**Synthesis, Characterization, and Polymerization of
Sulfonamide Based Bifunctional Monomers**

A thesis submitted in partial fulfillment of the
requirements for the degree of
Master of Science

By

BRADY HALL
B.S., The University of Southern Mississippi, 2014

2016

Wright State University

WRIGHT STATE UNIVERSITY
GRADUATE SCHOOL

July 26, 2016

I HEREBY RECOMMEND THAT THE THESIS PREPARED UNDER MY SUPERVISION BY Brady Hall ENTITLED Synthesis, Characterization, and Polymerization of Sulfonamide Based Bifunctional Monomers BE ACCEPTED IN PARTIAL FULFILLMENT OF THE REQUIREMENTS FOR THE DEGREE OF Master of Science.

Eric Fossum, Ph.D.
Thesis Advisor

Committee on
Final Examination

David Grossie, Ph.D.
Chair, Department of Chemistry

Eric Fossum, Ph.D.

William A. Feld, Ph.D.

Kenneth Turnbull, Ph.D.

Robert E. W. Fyffe, Ph.D.
Vice President for Research and
Dean of the Graduate School

ABSTRACT

Hall, Brady. M.S., Department of Chemistry, Wright State University, 2016. Synthesis, Characterization, and Polymerization of Sulfonamide Based Bifunctional Monomers.

A series of bifunctional monomers based on *N,N*-diallylbenzenesulfonamides with varying groups on the benzene moiety were investigated. The main goal of this project was to polymerize these monomers using radical and acyclic diene metathesis (ADMET) polymerization methods to polymerize through the allyl groups, and nucleophilic aromatic substitution (S_NAr) to polymerize through the fluorine groups on the phenyl ring.

Using phenyl substituted benzenesulfonyl chloride derivatives as a starting material, a series of *N,N*-diallylbenzenesulfonamide derivatives were prepared. The ADMET and radical cyclopolymerizations were monitored by 1H NMR spectroscopy, observing the disappearance of signals for the allyl groups in both, and the appearance of broad aliphatic signals in the radical cyclopolymers. The polymers formed via S_NAr reactions were followed by DEPT 90 ^{13}C NMR spectroscopy. Additionally, GPC, DSC, and TGA were used to characterize the polymers, which indicated successful cyclopolymerization, ADMET, and S_NAr reactions.

TABLE OF CONTENTS

1. INTRODUCTION	1
1.1. Radical Polymerization	1
1.1.1. Free Radical Polymerization (FRP)	1
1.1.2. Atom Transfer Radical Polymerization (ATRP).....	3
1.1.3. Initiators for Constant Activator Regeneration (ICAR) ATRP	4
1.1.4. Reversible Addition-Fragmentation Chain Transfer (RAFT) Polymerization.....	5
1.2. Acyclic Diene Metathesis (ADMET) Polymerization	6
1.3. Cyclopolymerization	7
1.4. Nucleophilic Aromatic Substitution (S_NAr) Polycondensation	9
1.5. Bifunctional Monomers.....	12
1.6. Introduction of Functionality	12
1.7. Current Research	13
2. EXPERIMENTAL.....	15
2.1. Materials.....	15
2.2. Instrumentation.....	16
2.3. General Procedure for the Synthesis of <i>N,N</i> -diallylbenzenesulfonamide (DABSA) Derivatives	17
2.4. General Procedure for the Synthesis of <i>N,N</i> -dioctylbenzenesulfonamide (DOctBSA) Derivatives	19
2.5. Radical Polymerization	21
2.5.1. FRP of DABSA Derivatives.....	21
2.5.2. ATRP of DABSA Derivatives	22

2.5.3. ICAR ATRP of DABSA Derivatives.....	23
2.5.4. Reversible Addition-Fragmentation Chain Transfer (RAFT) Polymerization of DABSA-2,4-DF	23
2.6. ADMET Polymerization of DABSA Derivatives	24
2.7. S _N Ar Copolymerization of 2a/b and 1d/e using 4,4'-dihydroxydiphenyl ether	25
2.8. Characterization.....	26
2.8.1. Size Exclusion Chromatography (SEC)	26
2.8.2. Differential Scanning Calorimetry (DSC).....	26
2.8.3. Thermogravimetric Analysis (TGA)	27
3. RESULTS AND DISCUSSION	28
3.1. Monomer Synthesis.....	28
3.1.1. Synthesis of <i>N,N</i> -diallylbenzenesulfonamide (DABSA) Derivatives	29
3.1.2. Synthesis of <i>N,N</i> -dioctylbenzenesulfonamide Derivatives	33
3.1.3. Spartan Calculations.....	37
3.1.4. Free Radical Polymers.....	39
3.1.5. ATRP and ICAR ATRP Polymers	43
3.1.6. RAFT of DABSA-2,4-DF	45
3.2. ADMET Polymers.....	46
3.3. S _N Ar Copolymers	51
3.3.1. S _N Ar Copolymerization of 1d and 2a using 4,4'-dihydroxydiphenyl ether	52
3.4. Polymer Molecular Weights and Thermal Properties	55

4.	CONCLUSIONS	65
5.	FUTURE WORK.....	67
6.	REFERENCES.....	68

LIST OF FIGURES

Figure 1. Di- and tri-thiocarbonylthio RAFT agents.	5
Figure 2. Commercially available PAES.	10
Figure 3. Examples of bifunctional monomers.	12
Figure 4. 300 MHz ^1H NMR spectrum (CDCl_3) of 1a	30
Figure 5. 300 MHz NMR spectra (CDCl_3) of the aromatic region of 1a-e	31
Figure 6. 75.7 MHz DEPT 135 (top) and ^{13}C NMR (bottom) spectral overlay (CDCl_3) of DABSA.	32
Figure 7. 75.5 MHz ^{13}C NMR spectral overlay (CDCl_3) of DABSA derivatives.	33
Figure 8. ^1H NMR spectral overlay (CDCl_3) of 2a (top) and 2b (bottom).	35
Figure 9. 75.5 MHz DEPT 135 (top) and ^{13}C (bottom) NMR spectral overlay (CDCl_3) of 2a	36
Figure 10. 75.5 MHz DEPT 135 (top) and ^{13}C NMR (bottom) spectral overlay (CDCl_3) of 2b	37
Figure 11. Electron density mapping of starting materials.	38
Figure 12. 300 MHz ^1H NMR spectral overlay (CDCl_3) of AIBN initiated p1a-e	42
Figure 13. 300 MHz ^1H NMR spectral overlay (CDCl_3) of BPO initiated p1a, d, and e	43
Figure 14. 300 MHz ^1H NMR spectra of 1d (top) and p2d (bottom).	46
Figure 15. 300 MHz ^1H NMR spectral overlay (CDCl_3) of 1a (top) and p3a (bottom).	48
Figure 16. 300 MHz ^1H NMR spectral overlay (CDCl_3) of ADMET polymers p3a-e	49
Figure 17. 75.5 MHz ^{13}C NMR spectra (CDCl_3) of 1a (top) and p3a (bottom).	50
Figure 18. 75.5 MHz ^{13}C NMR spectral overlay (CDCl_3) of ADMET polymers p3a-e	51

Figure 19. 300 MHz ^1H NMR (CDCl_3) spectral overlay of p4a (top) and p4b (bottom).	53
Figure 20. 75.5 MHz DEPT 90 ^{13}C NMR (CDCl_3) spectral overlay of 1d (top) and p4a (bottom).	54
Figure 21. 75.5 MHz DEPT 90 ^{13}C NMR (CDCl_3) spectral overlay of 1e (top) and p4b (bottom).	54
Figure 22. DSC results of AIBN initiated DABSA derivatives.	57
Figure 23. TGA results of AIBN initiated DABSA derivatives.	58
Figure 24. DSC results of BPO initiated DABSA derivatives.	58
Figure 25. TGA results of BPO initiated DABSA derivatives.	59
Figure 26. DSC results of ADMET polymers.	61
Figure 27. TGA results of 1c and p3c .	61
Figure 28. TGA results of ADMET Polymers.	62
Figure 29. DSC results of $\text{S}_\text{N}\text{Ar}$ copolymers.	63
Figure 30. TGA results of $\text{S}_\text{N}\text{Ar}$ copolymers.	64

LIST OF SCHEMES

Scheme 1. Radical formation in the radical initiators AIBN and BPO.	1
Scheme 2. Head and tail addition.	2
Scheme 3. Mechanism of the free radical polymerization of styrene.	2
Scheme 4. General mechanism of ATRP.	4
Scheme 5. Generally accepted mechanism for RAFT polymerization.	6
Scheme 6. Mechanism of ADMET polymerization.	7
Scheme 7. Cyclization of quaternary amines.	8
Scheme 8. Degradative chain transfer.	8
Scheme 9. General mechanism for S_NAr	10
Scheme 10. Outline of S_NAr polycondensation.	11
Scheme 11. Synthesis of PAEs via <i>meta</i> -activated S_NAr polycondensation reactions. ...	11
Scheme 12. Introducing functionality via pre and post polymerization modification.	13
Scheme 13. Pre (top) and post (bottom) polymerization modification of DABSA-4-Br. 14	
Scheme 14. Pre (top) and post (bottom) polymerization modification of DABSA-3,5-DF.	14
Scheme 15. Synthetic route for DABSA derivatives.	28
Scheme 16. Synthetic route for DOctBSA derivatives.	34
Scheme 17. General outline of the FRP of DABSA derivatives.	40
Scheme 18. ATRP of 1a-e	44
Scheme 19. ICAR ATRP of 1a-e	45
Scheme 20. RAFT polymerization of 1d	45
Scheme 21. ADMET polymerization of monomers 1a-e	47

Scheme 22. S_NAr copolymerization of **2a/b** and **1d/e** to form **p4a/b**. 52

LIST OF TABLES

Table 1. Literature values for diallylamine derivatives.....	9
Table 2. Calculated electrostatic charges of diallylamine derivatives.	38
Table 3. Differences in chemical shift and molecular weights of free radical polymers. 56	
Table 4. Thermal data for free radical polymers.....	57
Table 5. Molecular weight of RAFT polymer p2d	59
Table 6. Molecular weights and thermal properties of ADMET polymers.	60
Table 7. Molecular weights and thermal properties of S _N Ar polymers.	62

ACKNOWLEDGEMENTS

I would first like to express my gratitude to my advisor, Dr. Eric Fossum for his guidance and encouragement during my sojourn in his group. His patience and geniality has inspired me as a chemist, and most importantly as a person. I will be forever grateful to him for giving me this opportunity.

I would also like to thank my committee members Dr. William Feld and Dr. Kenneth Turnbull for their suggestions and assistance toward this thesis. Additionally, I would like to thank Luke Meyer for his invaluable assistance, as well as the past and present members of the Fossum research group, and the faculty and staff members of the Wright State University Department of Chemistry.

This work is based upon work supported by the National Science Foundation under CHE-1307117.

DEDICATION

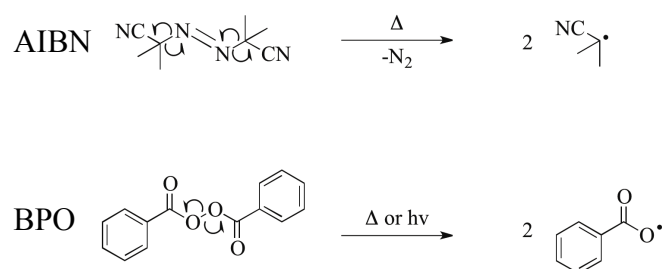
I would like to dedicate this work to my parents, Jodie and Steve Sartin, and Kenneth and Melissa Hall, as well as my grandparents, Helen and Gene Spence. Their continued love and support has pushed me to strive for my best. I would also like to dedicate this work to my partner, Katy Gaines, who has stood beside me during this demanding time in my life. I can't figure out if it's an end, or the beginning, but I know you all will be right there with me. Thank you.

1. INTRODUCTION

1.1. Radical Polymerization

1.1.1. Free Radical Polymerization (FRP)

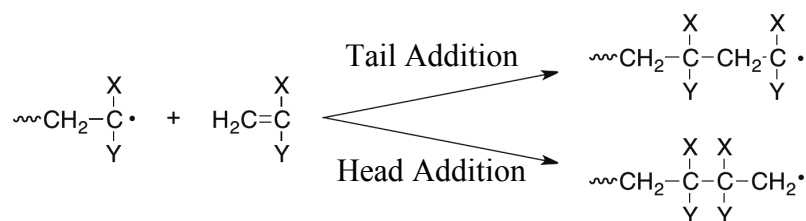
Radicals are chemical species that possess an unpaired electron in an outer shell, sometimes called a free spin, which gives rise to the term “free radical”. Free radical polymerization (FRP) is a type of chain growth polymerization, meaning that a high molecular weight polymer is formed early in the reaction. FRP is most commonly conducted on compounds with a carbon-carbon double bond using a radical initiator, such as 2,2'-azobis(2-methylpropionitrile) (AIBN) or benzoyl peroxide (BPO). The radicals are formed through either thermal or photochemical decomposition (see **Scheme 1**), and add to a monomer molecule by opening the π -bond to form a new radical center. This process is repeated many times as more monomer molecules are added to the propagating radical center.



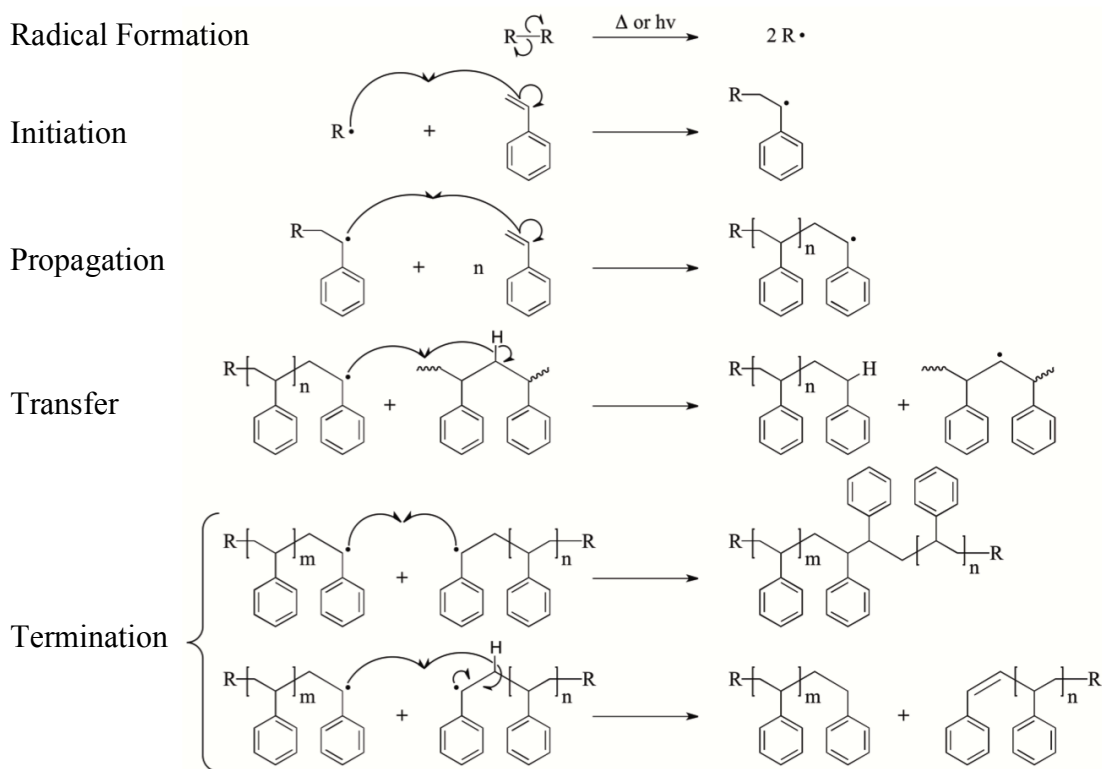
Scheme 1. Radical formation in the radical initiators AIBN and BPO.

Substitution at a radical center almost always increases stability by reducing the bond dissociation energy, and as such radical stability typically increases from

methyl < primary < secondary < tertiary. Normally this results in the addition of a radical to the less highly substituted end of asymmetrically substituted compounds (*i.e.* they predominantly result in tail addition, as shown in **Scheme 2**). Due to the high concentration of radical species in the system, the growing polymer chain is terminated by the destruction of the reactive center through hydrogen abstraction or some type of coupling, as illustrated in **Scheme 3**.



Scheme 2. Head and tail addition.



Scheme 3. Mechanism of the free radical polymerization of styrene.

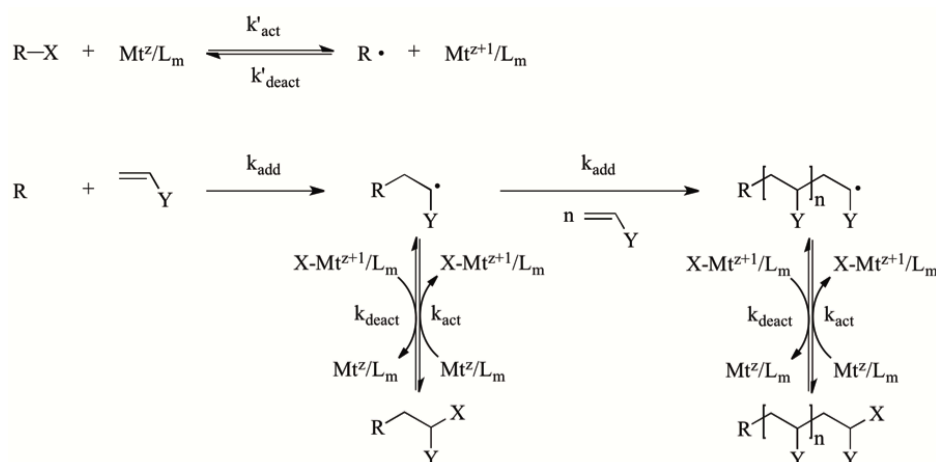
Owing to the high rate of termination in FRP, a narrow distribution of molecular weights cannot be achieved, and the dispersity (\bar{D}) is greater than 1.5.¹ In order to address this issue, methods of limiting the concentration of active radical species were investigated. Various types of controlled radical polymerization (CRP) techniques were developed, all of which owe their success to the persistent radical effect; a type of self-regulation of the two types of radical species (propagating and persistent) by some sort of mediating complex.²

1.1.2. Atom Transfer Radical Polymerization (ATRP)

Atom Transfer Radical Polymerization (ATRP), first reported in 1995 from the laboratories of Sawamoto,³ Matyjaszewski,⁴ and Percec,⁵ was the first true CRP technique. Previous attempts include iniferter and nitroxide-mediated radical polymerization (NMP) methods, both of which have only limited success in facilitating radical polymerizations. Both iniferter and NMP have a limited selection of monomers from which to choose, and iniferter polymerization further suffers from broad \bar{D} and limited block copolymer formation. ATRP does not have these issues, and can be tailored for specific reactions by modifying one of the reagents involved: the halogenated initiator, transition metal compound, or nitrogen based ligand.

In ATRP, a transition metal compound in its lower oxidative state (*e.g.* copper (I) bromide) is used to mediate a reversible redox process and establish equilibrium between propagating and persistent radicals.¹ This reversible process results in control of the radical species by deactivating the radical center, causing low radical concentration and minimizing termination of the growing polymer chain. The success of an ATRP is contingent on fast and quantitative initiation of the monomers so that all of the

propagating species grow simultaneously; resulting in a narrow \bar{D} . ATRP is traditionally conducted on vinyl monomers, with ratios of monomer:catalyst:initiator in the range of 100:1:1 to 100:1:10 and can be conducted in bulk, solution, or various heterogeneous media including suspension, dispersion and aqueous emulsion.⁶



Scheme 4. General mechanism of ATRP.⁷

1.1.3. Initiators for Constant Activator Regeneration (ICAR) ATRP

While ATRP is a very versatile polymerization method, it is not applicable for every type of situation. Initiators for constant activator regeneration (ICAR) ATRP is one technique that has been developed to address these limitations. Unlike ATRP, ICAR ATRP utilizes a transition metal compound in a higher oxidative state, (*e.g.* a copper (II) halide) as well as a traditional radical initiator (*e.g.* AIBN or BPO). The initiator generates radicals that react with the transition metal complex to continuously regenerate its lower oxidative state, preventing it from being consumed in termination reactions. This allows for use of the catalyst at concentrations between 10-50 ppm, and is beneficial in situations where removal or recycling of the catalyst is not possible.⁸

1.1.4. Reversible Addition-Fragmentation Chain Transfer (RAFT) Polymerization

Another prominent type of CRP is reversible addition-fragmentation chain transfer (RAFT) polymerization, which was developed in 1996 by a team at Commonwealth Scientific and Industrial Research Organisation (CSIRO).⁹ In RAFT polymerization, the propagating and persistent radical equilibrium is mediated by a di- or trithiocarbonylthio RAFT agent.

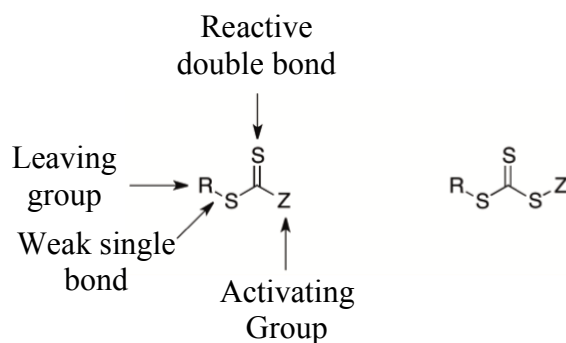
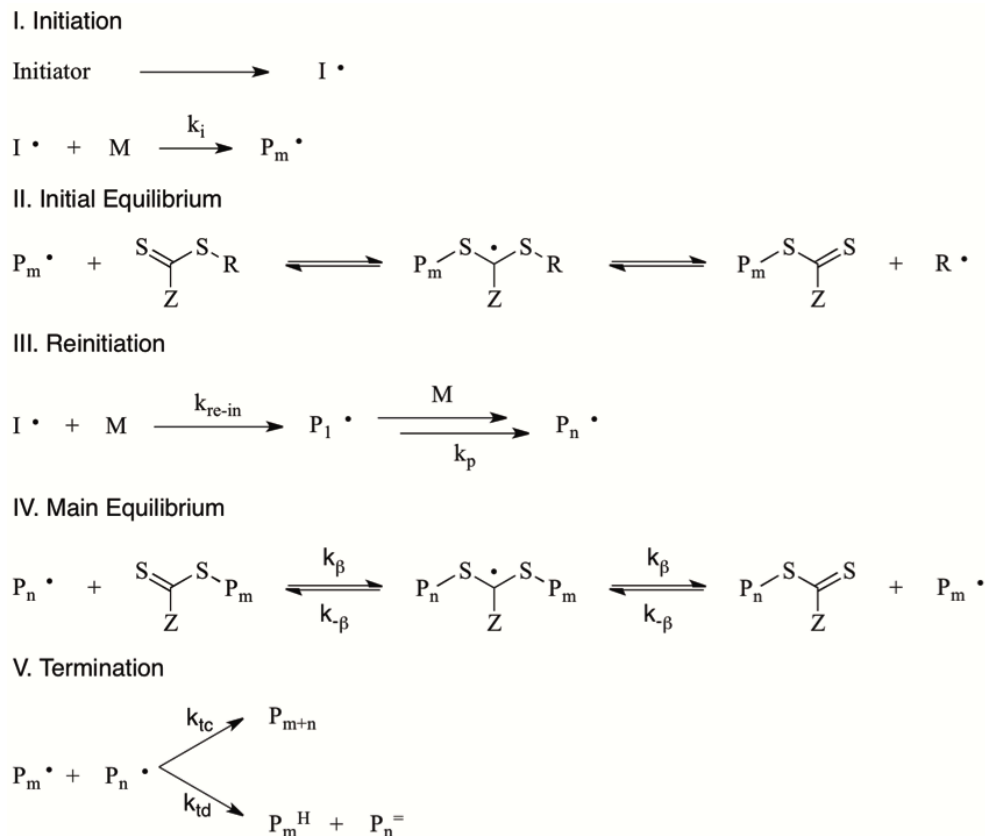


Figure 1. Di- and tri-thiocarbonylthio RAFT agents.

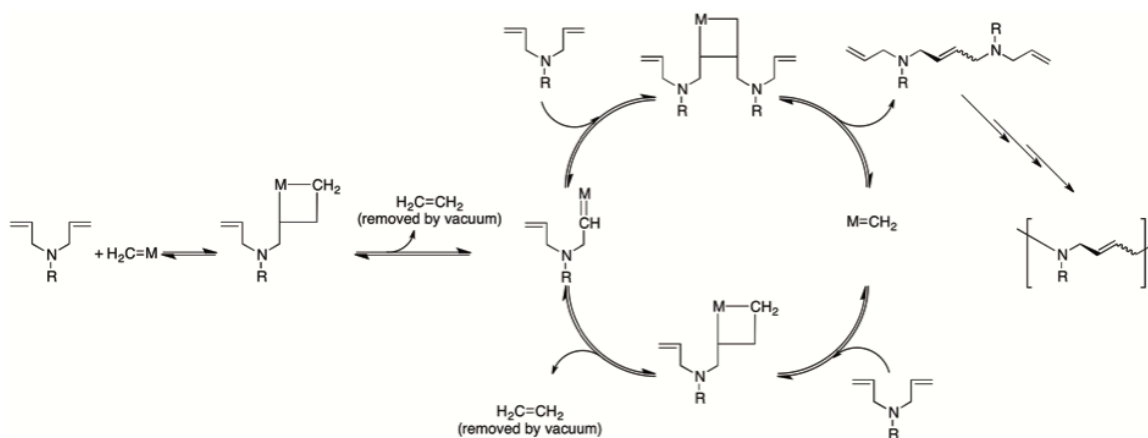
RAFT owes its success to a sequence of addition-fragmentation equilibria, shown in **Scheme 5**. Early in the polymerization, the propagating radical adds to the thiocarbonylthio compound, which results in fragmentation of the intermediate radical species (Step II). This yields a polymeric thiocarbonylthio compound (P_m^\bullet) as well as a new radical species, which can further react with more monomer forming a new propagating radical species (P_n^\bullet). A rapid equilibrium is established between the active propagating radicals (P_m^\bullet and P_n^\bullet) that provide an equal probability for all chains to grow, allowing for the formation of polymers with a narrow D .¹⁰



Scheme 5. Generally accepted mechanism for RAFT polymerization.

1.2. Acyclic Diene Metathesis (ADMET) Polymerization

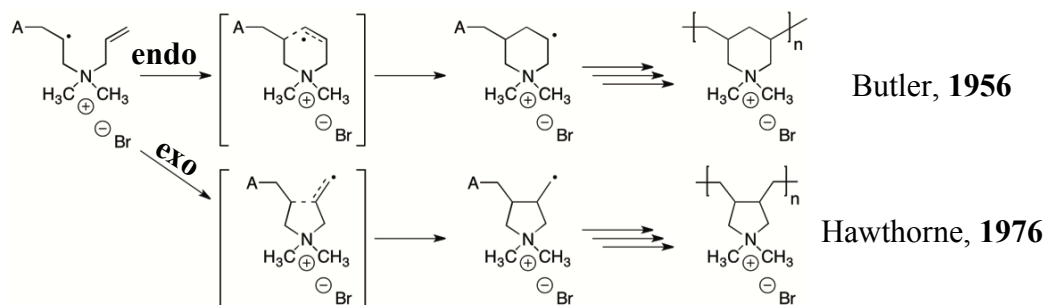
Acyclic diene metathesis (ADMET) polymerization is a type of step-growth, condensation polymerization, and was developed in 1991 by Dr. Ken Wagener at the University of Florida. In ADMET polymerization, a transition metal catalyst is used to polymerize terminal dienes to polyenes. Polymer formation is driven by the liberation of ethylene gas, with the double bonds formed either in a *cis*- or *trans*-configuration, depending on the monomer and catalyst structure.



Scheme 6. Mechanism of ADMET polymerization.

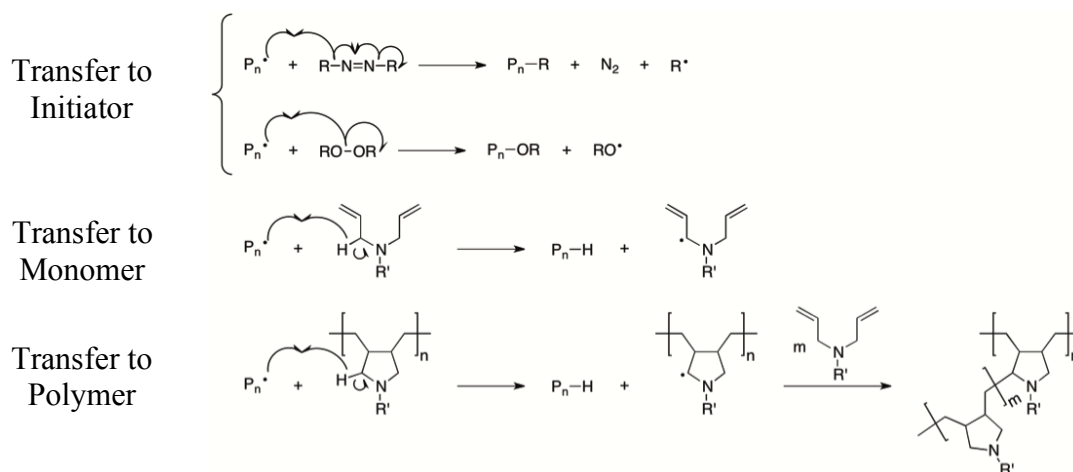
1.3. Cyclopolymerization

Alternating intra-intermolecular polymerization, more commonly known as cyclopolymerization, is a type of polymerization in which cyclic species are formed from the intramolecular cyclization of monomers containing unconjugated dienes. This type of polymerization was first introduced by Butler and coworkers, who demonstrated that the radical polymerization of *N,N*-diallyl-*N,N*-dimethylammonium chloride (DADMAC) yielded soluble, uncrosslinked polymers with little to no unsaturation.¹¹ Though Butler believed that he had formed a six-membered (endo cyclized) species, Hawthorn et al. demonstrated that the route through which the polymer was formed yielded a five-membered (exo cyclized) species due to more favorable orbital overlap in the transition state,¹² as shown in **Scheme 7**.



Scheme 7. Cyclization of quaternary amines.

Although diallyl quaternary ammonium salts cyclopolymerize to a relatively high efficiency, diallyl tertiary amines do not readily cyclopolymerize,¹³ in part due to degradative chain transfer, a chain-breaking reaction involving the abstraction of hydrogen or some other atom or species, *i.e.* initiator, monomer, or polymer.¹⁴ This decreases the size of the propagating polymer species, and results in a branched polymer system when chain transfer to polymer occurs. However, Zubov et al. suggested that a strong electron withdrawing substituent on diallyl tertiary amines induces a strong partial positive charge on the nitrogen atom, decreasing the effects of degradative chain transfer.¹⁵

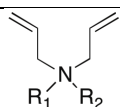


Scheme 8. Degradative chain transfer.

Due to the strong electron withdrawing nature of the sulfone group, a partial positive charge is induced on the nitrogen in diallyl tertiary sulfonamides, which should

increase their ability to polymerize. Indeed, J. H. Hodgkin *et al.* successfully radically polymerized tertiary diallyl sulfonamides with methyl and phenyl substituents in bulk.¹⁶ It has also been shown that the smaller the difference in chemical shifts of the terminal and penultimate alkene carbons or hydrogens, the greater the cyclization efficiency and greater the molecular weight of the resulting polymer,¹⁷ and is indicative of a greater partial positive charge on the nitrogen.

Table 1. Literature values for diallylamine derivatives.

		% Conversion to Polymer
R ₁	R ₂	
-H	-	Trace ¹⁶
-H	-H	70 ¹⁸
-CH ₃	-	24 ¹⁹
-CH ₃	-CH ₃	80 ²⁰
-CN	-	22 ¹⁶
-SO ₂ C ₆ H ₅	-	30 ¹⁶
-SO ₂ C ₆ H ₄ Cl	-	36 ²¹

1.4. Nucleophilic Aromatic Substitution (S_NAr) Polycondensation

Poly(arylene ether sulfone)s (PAES) are a class of amorphous engineering thermoplastics, and can be prepared by either electrophilic aromatic substitution,²² or nucleophilic aromatic substitution (S_NAr) polycondensation.²³ Today, the S_NAr route of polycondensation is most commonly utilized for the commercial production of these thermoplastics, and a few of the commercially available PAES are shown in **Figure 2**. The mechanism of S_NAr involves the activation of an aryl halide by an electron-withdrawing group (EWG), typically located in the *para*-position, as shown in **Scheme 9**.

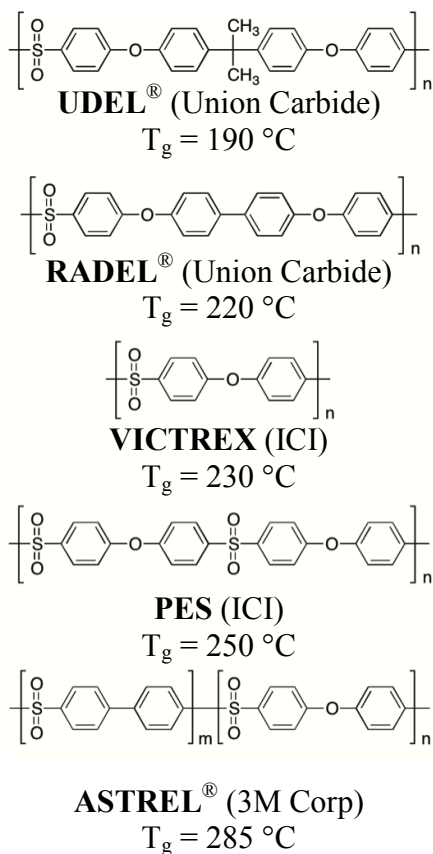
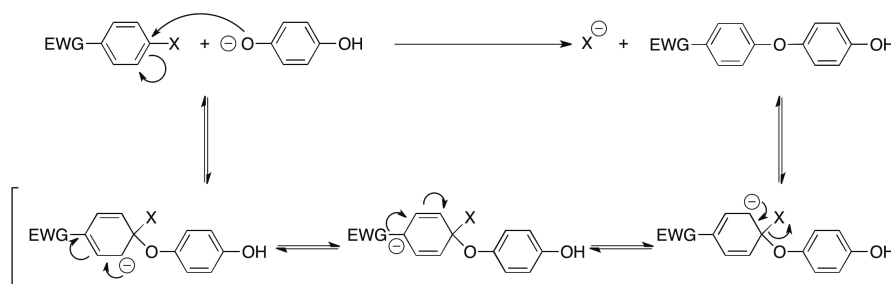
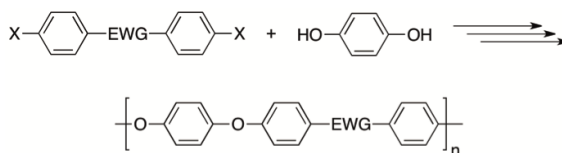


Figure 2. Commercially available PAES.

The first step in a S_NAr mechanism is largely thought to be reversible and the rate-determining step: a nucleophilic attack at the *ipso* carbon resulting in a Meisenheimer complex, a resonance stabilized anionic intermediate species. The second step involves the loss of the halide group, resulting in the benzene regaining its aromaticity.

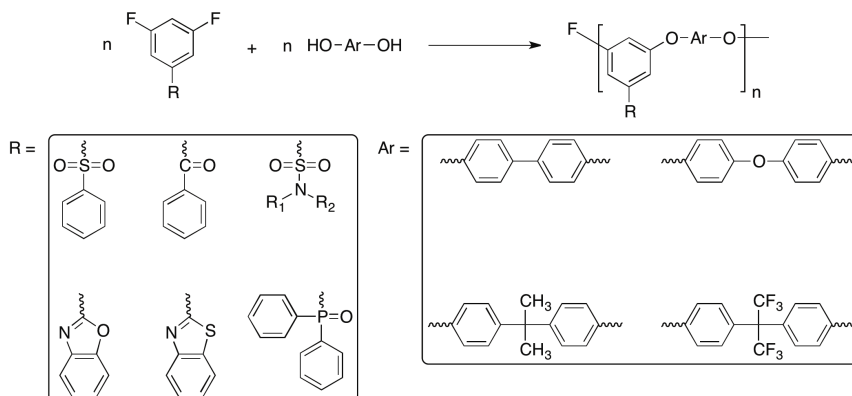


Scheme 9. General mechanism for S_NAr.



Scheme 10. Outline of S_NAr polycondensation.

Although S_NAr reactions are usually carried out with aryl halides activated by an EWG in the *ortho*- or *para*- position, Kaiti *et al.* demonstrated that S_NAr can also take place at the *meta* position relative to the EWG.²⁴ Since then, our group has introduced a variety of activating groups for the synthesis of PAEs via *meta* activated S_NAr reactions,²⁵⁻²⁷ as shown in **Scheme 11**. In these systems, the activating group resides pendent to the polymer backbone, allowing for the introduction of various functional groups without directly modifying the backbone of the polymer.



Scheme 11. Synthesis of PAEs via *meta*-activated S_NAr polycondensation reactions.

Sulfonamides have been described as strong electron withdrawing groups for the activation of aryl halides for S_NAr reactions when positioned *ortho* and *para*,²⁸ as well as *meta*, to the halide.^{27,29} As a site for the introduction of a variety of functional groups pendent to the polymer chain, sulfonamides are an attractive option. This feature can be exploited to tailor the properties of the polymer for a specific application.

1.5. Bifunctional Monomers

Bifunctional monomers are compounds that have two distinct types of functionality with mutually exclusive reactivity. That is to say, polymerization of one type of functional group does not affect the other. Current methods of polymerizing bifunctional monomers make use of anionic, cationic, and radical polymerization methods, examples of which are shown in **Figure 3**.

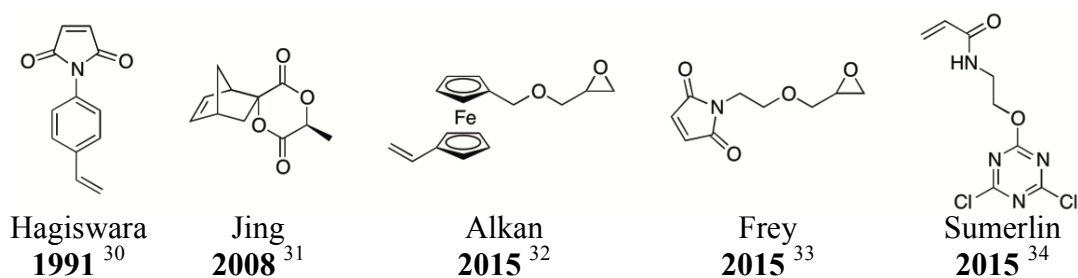
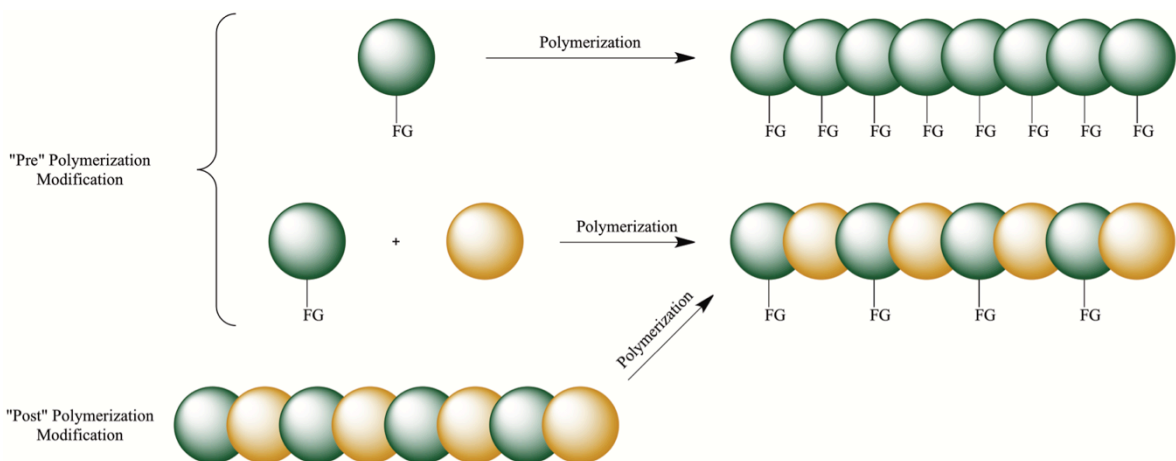


Figure 3. Examples of bifunctional monomers.

1.6. Introduction of Functionality

In order to meet a specific application need, it is a useful tool to tailor the physical and chemical properties of a polymer through introduction of functional groups to the system. This can be achieved in one of two ways: by either introducing functionality at the monomer stage (pre), or by introducing functionality after the polymerization has been completed (post). A general scheme for the introduction of functional groups is shown in **Scheme 12**.



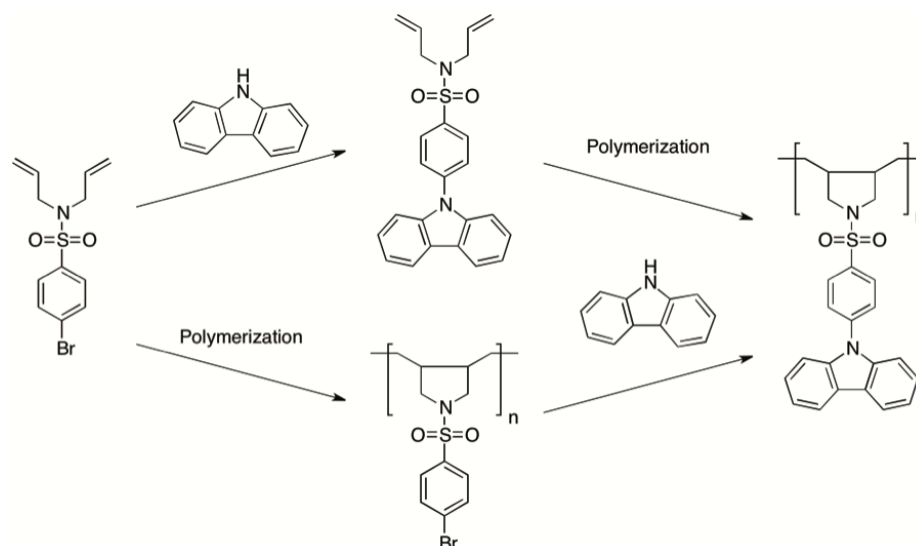
Scheme 12. Introducing functionality via pre and post polymerization modification.

1.7. Current Research

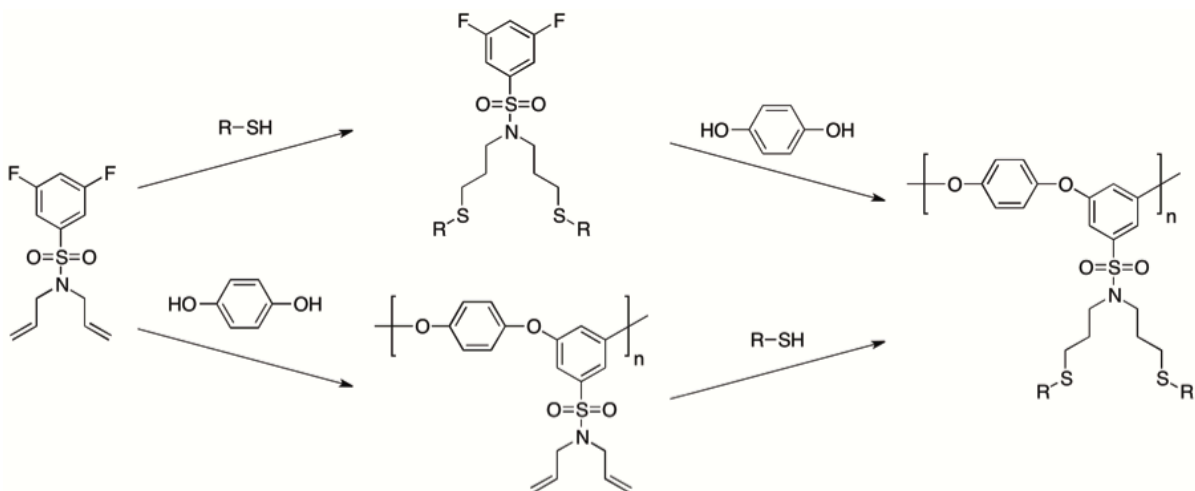
In this project, the sulfonamide moiety was exploited in order to form bifunctional monomers that were capable of undergoing S_NAr polycondensation, as well as metathesis and various forms of radical polymerizations. A series of *N,N*-diallylbenzenesulfonamide based monomers were prepared in a one-step process modified from the literature, as shown in **Scheme 15**. These monomers are able to be utilized for both pre-and post polymerization functionalization, and provide a straightforward way of tuning the physical properties of a polymer by changing the ratio of the selected monomer.

In order to take advantage of both systems (pre or post polymerization modification), as well as the bifunctionality of these monomers, the type of modification, as well as the type of polymerization (radical, ADMET, or S_NAr) can be varied to produce a wide variety of polymers. For post-polymerization functionalization of a polymer formed by either radical or ADMET polymerization, an inactive functional group, such as bromine, can be introduced at the monomer level then converted by post-polymerization modification (**Scheme 13**). Conversely, polymers formed via S_NAr can be

post functionalized by reacting the pendent allyl groups with an appropriate compound, e.g. a thiol compound (**Scheme 14**).



Scheme 13. Pre (top) and post (bottom) polymerization modification of DABSA-4-Br.



Scheme 14. Pre (top) and post (bottom) polymerization modification of DABSA-3,5-DF.

2. EXPERIMENTAL

2.1. Materials

Diethyl ether and toluene were purchased from Fischer Scientific and used as received. 4-Fluorobenzenesulfonyl chloride, 2,4-difluorobenzenesulfonyl chloride and 3,5-difluorobenzenesulfonyl chloride were purchased from Oakwood Chemicals and used as received. 2,2'-Azobis(2-methylpropionitrile) (AIBN), benzenesulfonyl chloride, 4-bromobenzenesulfonyl chloride, benzoyl peroxide (BPO), chloroform-*d* (CDCl₃), copper (I) bromide (CuBr), copper (II) bromide (CuBr₂), diallylamine, dioctylamine, ethyl-2-bromopropionate (EBrP), Hoveyda-Grubbs 2nd generation catalyst (HG2G), hydrochloric acid (HCl), *N,N,N',N',N''*-pentamethyldiethylenetriamine (PMDETA), triethylamine (TEA), tris[2-(dimethylamino)ethyl]amine (Me₆TREN), and cyanomethyl methyl(phenyl) carbamodithioate (CMMPCDT), were purchased from Sigma-Aldrich and used as received. 4,4'-dihydroxydiphenyl ether was purchased from TCI Chemicals and recrystallized from toluene and dried under vacuum prior to use. Calcium hydride (CaH₂) and potassium carbonate (K₂CO₃) were purchased from Sigma-Aldrich and dried in an oven at 130 °C before use. Dichloromethane (DCM) and xylenes were purchased from Fischer Scientific; *N*-methyl-2-pyrrolidone (NMP) was purchased from Sigma-Aldrich, all were dried over CaH₂ and distilled prior to use.

2.2. Instrumentation

Differential Scanning Calorimetry (DSC) and Thermogravimetric Analysis (TGA) analyses were carried out on a TA Instruments DSC Q200 (under nitrogen) and TGA Q500 (under nitrogen or air), respectively at a heating rate of 10 °C/min. Gas chromatography-mass spectroscopy (GC/MS) analyses were performed using an Agilent Technologies 7820A Series GC System, and an Agilent Technologies 5975 Mass Selective Detector/Quadrupole system. ^1H and ^{13}C Nuclear Magnetic Resonance (NMR) spectra were acquired using a Bruker AVANCE 300 MHz instrument operating at 300 and 75.5 MHz, respectively. Samples were dissolved in CDCl_3 at a concentration of (~ 30 mg /0.7 mL). Gel permeation chromatography (GPC) analysis was performed using instrumentation consisting of a Viscotek Model 270 dual detector (viscometer and light scattering) and a Viscotek Model VE3580 refractive index detector. Two Polymer Laboratories 5 μm PLgel Mixed-C columns (heated to 35 °C) were used with THF/5% (v/v) acetic acid as the eluent and a GPC max VE-2001 with pump operating at 1.0 mL/minute. Cyclization efficiencies (CE) were determined by integrating the double bond proton peaks relative to the backbone proton peaks in the ^1H NMR spectrum. Weight average molecular weights, M_w , and Dispersity (D) values were determined using OmniSec software (calibrated with polystyrene standards). Melting points were determined on a MEL-TEMP apparatus, or DSC and are uncorrected. Elemental analyses were obtained from Midwest Microlabs, Inc., Indianapolis, IN. The energy of monomers **1a-e** was calculated in vacuum using the Spartan' 10 computational software package (Wavefunction, Inc., Irvin, CA). The geometries were initially optimized using the semiempirical method RM1, and then further optimized using density functional theory at

the B3LYP/6-31+G** level. The energy of each of the monomers was recorded and expressed as a relative energy with respect to the most stable species of that charge.

2.3. General Procedure for the Synthesis of *N,N*-diallylbenzenesulfonamide (DABSA) Derivatives

The general procedure for the synthesis of *N,N*-diallylbenzenesulfonamide (DABSA) derivatives will be illustrated using *N,N*-diallylbenzenesulfonamide.

To a solution of benzenesulfonyl chloride (4.00 g, 22.6 mmol) in 70 mL of dichloromethane, was added triethylamine (TEA, 3.95 mL, 28.3 mmol, 25% excess). The solution was allowed to stir for five minutes, at which point diallylamine (3.62 mL, 28.31 mmol, 25% excess) was added and the resulting mixture stirred for approximately three hours, during which time a mild exothermic reaction occurred. Analysis of an aliquot by GC/MS showed quantitative conversion of the starting material to the desired product (if the GC/MS did not show quantitative conversion, TEA was added dropwise until TEA-HCl precipitated in the reaction mixture). The organic phase was extracted with 2 x 250 mL 10% HCl, 2 x 250 mL cold, distilled water, 1 x 100 mL 5% HCl, and 1 x 100 mL cold, distilled water, and then dried over MgSO₄ and filtered. The solvent was removed via rotary evaporation to afford 4.83 g (90%) of *N,N*-diallylbenzenesulfonamide (DABSA, **1a**) as a light yellow liquid (M.P. < -85 °C by DSC), ¹H-NMR (CDCl₃, δ): 3.84 (d, 4H, N-CH₂-), 5.13 (m, 2H, *cis* C=CH₂), 5.18 (m, 2H, *trans* C=CH₂), 5.62 (m, 2H, -CH=), 7.56 (m, 3H, Ar-H), 7.84 (m, 2H, Ar-H) ppm; DEPT 135 ¹³C NMR (CDCl₃, δ): 49.3 (s, N-CH₂-), 119.0 (s, =CH₂), 127.1 (s, Ar-H), 129.1 (s, Ar-H), 132.5 (s, -CH=), 132.5 (s, Ar-H) ppm. ¹³C NMR (CDCl₃, δ): 49.3 (s, -CH₂-), 119.0 (s, =CH₂), 127.1 (s, Ar-H), 129.1 (s, Ar-H), 132.5 (s, Ar-H), 132.5 (s, -CH=), 140.4 (s, Ar-SO₂) ppm.

Elemental Analysis: Calc. Anal. for C₁₂H₁₅NO₂S: C, 60.3; H, 6.37; Found: C, 60.8; H, 6.29.

Syntheses of the remaining *N,N*-diallylbenzenesulfonamides were carried out in a similar fashion, with the exception of *N,N*-diallyl-3,5-difluorobenzenesulfonamide which was precipitated from ethanol/water to afford a white solid.

N,N-diallyl-4-bromobenzenesulfonamide (DABSA-4-Br, **1b**, 96%): M.P. = -62 °C by DSC; ¹H-NMR (CDCl₃, δ): 3.76 (d, 4H, N-CH₂-), 5.10 (m, 2H, *cis* C=CH₂), 5.13 (m, 2H, *trans* C=CH₂), 5.56 (m, 2H, -CH=), 7.63 (m, 4H, Ar-H) ppm; DEPT 135 ¹³C NMR (CDCl₃, δ): 49.3 (s, N-CH₂-), 119.3 (s, =CH₂), 128.7 (s, Ar-H), 132.3 (s, Ar-H), 132.3 (s, -CH=) ppm. ¹³C NMR (CDCl₃, δ): 49.3 (s, -CH₂-), 119.3 (s, =CH₂), 127.3 (s, Ar-Br), 128.7 (s, Ar-H), 132.3 (s, Ar-H), 132.3 (s, -CH=), 139.5 (s, Ar-SO₂) ppm. Elemental Analysis: Calc. Anal. for C₁₂H₁₄NO₂SBr: C, 45.5; H, 4.46; Found: C, 45.7; H, 4.32.

N,N-diallyl-4-fluorobenzenesulfonamide (DABSA-4-F, **1c**, 86%): M.P. < -85 °C by DSC; ¹H-NMR (CDCl₃, δ): 3.79 (d, 4H, N-CH₂-), 5.10 (m, 2H, *cis* C=CH₂), 5.15 (m, 2H, *trans* C=CH₂), 5.58 (m, 2H, -CH=), 7.16 (m, 2H, Ar-H), 7.82 (m, 2H, Ar-H) ppm; DEPT 135 ¹³C NMR (CDCl₃, δ): 49.3 (s, N-CH₂-) 116.1 (d, Ar-H), 119.2 (s, =CH₂), 129.8 (d, Ar-H), 132.3 (s, -CH=) ppm. ¹³C NMR (CDCl₃, δ): 49.3 (s, -CH₂-), 116.1 (s, Ar-H), 119.2 (s, =CH₂), 129.8 (d, Ar-H), 132.3 (s, -CH=), 136.4 (s, Ar-SO₂), 166.4 (d, Ar-F) ppm. Elemental Analysis: Calc. Anal. for C₁₂H₁₄NO₂SF: C, 56.5; H, 5.53; Found: C, 56.5; H, 5.45.

N,N-diallyl-2,4-difluorobenzenesulfonamide (DABSA-2,4-DF, **1d**, 94%): M.P. < -85 °C by DSC; ¹H-NMR (CDCl₃, δ): 3.92 (d, 4H, N-CH₂-), 5.15 (m, 2H, *cis* C=CH₂),

5.19 (m, 2H, *trans* C=CH₂), 5.64 (m, 2H, -CH=), 6.95 (m, 2H, Ar-H), 7.94 (m, 1H, Ar-H) ppm; DEPT 135 ¹³C NMR (CDCl₃, δ): 49.1 (s, N-CH₂-), 105.6 (t, Ar-H), 111.7 (dd, Ar-H), 119.2 (s, =CH₂), 132.3 (s, -CH=), 132.5 (d, Ar-H) ppm. ¹³C NMR (CDCl₃, δ): 49.1 (d, -CH₂-), 105.6 (t, Ar-H), 111.6 (d, Ar-H), 119.2 (s, =CH₂), 125.4 (m, Ar-SO₂), 132.3 (s, -CH=), 132.5 (d, Ar-H) 159.5 (dd, Ar-F), 165.6 (dd, Ar-F) ppm. Elemental Analysis: Calc. Anal. for C₁₂H₁₃NO₂SF₂: C, 52.7; H, 4.79; Found: C, 52.3; H, 4.63.

N,N-diallyl-3,5-difluorobenzenesulfonamide (DABSA-3,5-DF, **1e**, 93%): M.P. = 45.5-48 °C; ¹H-NMR (CDCl₃, δ): 3.86 (d, 4H, N-CH₂-), 5.18 (m, 2H, *cis* C=CH₂), 5.22 (dq, 2H, *trans* C=CH₂), 5.64 (m, 2H, -CH=C), 7.03 (tt, 1H, Ar-H), 7.37 (m, 2H, Ar-H); DEPT 135 ¹³C NMR (CDCl₃, δ): 49.4 (s, N-CH₂-), 108.0 (t, Ar-H), 110.6 (dd, Ar-H), 119.6 (s, =CH₂), 131.9 (s, -CH=) ppm. ¹³C NMR (CDCl₃, δ): 49.4 (s, -CH₂-), 108.0 (t, Ar-H), 110.6 (dd, Ar-H), 119.6 (s, =CH₂), 131.9 (s, -CH=), 143.9 (t, Ar-SO₂) 162.8 (dd, Ar-H) ppm. Elemental Analysis: Calc. Anal. for C₁₃H₁₄NO₂SF₂: C, 52.74; H, 4.79; Found: C, 52.8; H, 4.67.

2.4. General Procedure for the Synthesis of *N,N*-dioctylbenzenesulfonamide

(DOctBSA) Derivatives

The general procedure for the synthesis of *N,N*-dioctylbenzenesulfonamide derivatives will be illustrated using *N,N*-dioctyl-2,4-difluorobenzenesulfonamide (**2a**).

To a solution of 2,4-difluorobenzenesulfonyl chloride (4.00 g, 22.6 mmol) in 70 mL of dichloromethane, was added triethylamine (TEA, 3.95 mL, 28.3 mmol, 25% excess). The solution was allowed to stir for five minutes, at which point dioctylamine (3.62 mL, 28.31 mmol, 25% excess) was added and the resulting mixture stirred for approximately three hours, during which time a mild exothermic reaction occurred.

Analysis of an aliquot by GC/MS showed quantitative conversion of the starting material to the desired product (if the GC/MS did not show quantitative conversion, TEA was added dropwise until TEA-HCl precipitated in the reaction mixture). The organic phase was extracted with 2 x 250 mL 10% HCl, 2 x 250 mL cold, distilled water, 1 x 100 mL 5% HCl, and 1 x 100 mL cold, distilled water, and then dried over MgSO₄ and filtered. Once the solvent was removed via rotary evaporation, approximately 25 mL of hexanes was added and the solution stirred for two hours. The dioctylamine precipitate was filtered off, and the solvent removed via rotary evaporation to afford 4.83 g (70%) of *N,N*-dioctyl-2,4-difluorobenzenesulfonamide (DOctBSA-2,4-DF, **2a**) as a light yellow liquid. ¹H-NMR (CDCl₃, δ): 0.89 (t, 6H, -CH₃), 1.28, (m, 20H, -CH₂-), 1.51 (m, 4H, -CH₂-), 3.23 (t, 4H, N-CH₂-), 6.96 (m, 2H, Ar-H), 7.93 (m, 1H, Ar-H) ppm. DEPT 135 ¹³C NMR (CDCl₃, δ): 13.9 (s, -CH₃), 22.5 (s, -CH₂-), 26.5 (s, -CH₂-), 28.4 (s, -CH₂-), 29.1 (s, -CH₂-), 29.1 (s, -CH₂-), 31.7 (s, -CH₂-), 49.5 (d, N-CH₂), 105.3 (t, Ar-H), 111.4 (dd, Ar-H), 132.4 (dd, Ar-H) ppm. ¹³C NMR (CDCl₃, δ): 13.9 (s, -CH₃), 22.5 (s, -CH₂-), 26.5 (s, -CH₂-), 28.4 (s, -CH₂-), 29.1 (s, -CH₂-), 29.1 (s, -CH₂-), 31.7 (s, -CH₂-), 49.5 (d, N-CH₂-), 105.3 (t, Ar-H), 111.4 (dd, Ar-H), 125.3 (dd, Ar-SO₂-), 132.4 (dd, Ar-H), 159.4 (dd, Ar-F), 165.3 (dd, Ar-F) ppm. Elemental Analysis: Calc. Anal. for C₂₂H₃₃NO₂SF₂: C, 63.3; H, 8.93; Found: C, 62.3; H, 8.55.

N,N-dioctyl-3,5-difluoronbenzenesulfonamide (DOctBSA-3,5-DF, **2b**, 70%): ¹H-NMR (CDCl₃, δ): 0.90 (t, 6H, -CH₃), 1.27 (m, 20H, -CH₂-), 1.53 (m, 4H, -CH₂-), 3.15 (t, 4H, N-CH₂-), 7.01 (tt, 1H, Ar-H), 7.35 (m, 1H, Ar-H) ppm. DEPT 135 ¹³C NMR (CDCl₃, δ): 14.0 (s, -CH₃), 22.6 (s, -CH₂-), 26.7 (s, -CH₂-), 28.6 (s, -CH₂-), 29.1 (s, -CH₂-), 31.7 (s, -CH₂-), 48.2 (s, N-CH₂-), 107.7 (t, Ar-H), 110.5 (dd, Ar-H) ppm. ¹³C NMR (CDCl₃, δ):

14.0 (s, -CH₃), 22.6 (s, -CH₂), 26.7 (s, -CH₂-), 28.6 (s, -CH₂-), 29.1 (s, -CH₂-), 31.7 (s, -CH₂-), 48.2 (s, N-CH₂-), 107.7 (t, Ar-H), 110.5 (dd, Ar-H), 143.7 (t, Ar-SO₂), 162.8 (dd, Ar-F) ppm. Elemental Analysis: Calc. Anal. for C₂₂H₃₃NO₂SF₂: C, 63.9; H, 8.04; Found: C, 63.1; H, 9.05.

2.5. Radical Polymerization

2.5.1. FRP of DABSA Derivatives

The general procedure for the free radical polymerization (FRP) of *N,N*-diallylbenzenesulfonamide (DABSA) derivatives will be illustrated using DABSA, with AIBN as the initiating species.

To a 25 mL Schlenk tube equipped with a magnetic stir bar was added DABSA (0.183 g, 7.75 mmol) and AIBN (0.191 g, 1.16 mmol, 15%). After purging with nitrogen for 25 minutes, the tube was lowered into an oil bath heated to 70 °C and allowed to react for 24 hours, after which point a highly viscous, dark yellow oil was observed. The polymer was precipitated from diethyl ether to afford 0.094 g (51%) of **p1a** as a white solid. ¹H NMR (CDCl₃, δ): 2.06 (m, 243H, Backbone -H), 3.83 (d, 4H, N-CH₂-), 5.15 (m, 4H, =CH₂), 5.61 (m, 2H, -CH=), 7.57 (s, 65H, Ar-H), 7.82 (s, 45H, Ar-H) ppm.

p1a (BPO, 49%) ¹H NMR (CDCl₃, δ): 1.97 (m, 503 H, Backbone-H), 3.83 (d, 4H, N-CH₂-), 5.15 (m, 4H, =CH₂), 5.61 (m, 2H, -CH=), 7.56 (s, 149H, Ar-H), 7.82 (s, 99H, Ar-H) ppm.

The FRP of the remaining DABSA derivatives were carried out in an analogous fashion

p1b (AIBN, 84%) ¹H NMR (CDCl₃, δ): 2.08 (m, 330H, Backbone-H), 3.83 (d, 4H, N-CH₂-), 5.17 (m, 2H, =CH₂), 5.59 (m, 4H, -CH=), 7.70 (m, 122H, Ar-H) ppm.

p1c (AIBN, 63%) ^1H NMR (CDCl_3 , δ): 2.05 (m, 285H, Backbone-H), 3.83 (d, 4H, N- CH_2 -), 5.16 (m, 4H, $=\text{CH}_2$), 5.62 (m, 2H, -CH=), 7.23 (m, 50H, Ar-H), 7.85 (m, 50H, Ar-H) ppm.

p1d (AIBN, 67%) ^1H NMR (CDCl_3 , δ): 2.19 (m, 869H, Backbone-H), 3.91 (d, 4H, N- CH_2 -), 5.17 (m, 4H, $=\text{CH}_2$), 5.63 (m, 2H, -CH=), 7.03 (s, 145H, Ar-H), 7.91 (s, 75H, Ar-H) ppm.

p1d (BPO, 58%) ^1H NMR (CDCl_3 , δ): 2.15 (m, 923H, Backbone-H), 3.92 (d, 4H, N- CH_2 -), 5.17 (m, 4H, $=\text{CH}_2$), 5.63 (m, 2H, -CH=), 7.01 (s, 164H, Ar-H), 7.91 (s, 85H, Ar-H) ppm.

p1e (AIBN, 90%) ^1H NMR (CDCl_3 , δ): 2.10 (m, 490H, Backbone-H), 3.86 (d, 4H, N- CH_2 -), 5.20 (m, 4H, $=\text{CH}_2$), 5.63 (m, 2H, -CH=), 7.09 (s, 42H, Ar-H), 7.36 (s, 92H, Ar-H) ppm.

p1e (BPO, 56%) ^1H NMR (CDCl_3 , δ): 2.12 (m, 509H, Backbone-H), 3.86 (d, 4H, N- CH_2 -), 5.19 (m, 4H, $=\text{CH}_2$), 5.64 (m, 2H, -CH=), 7.08 (s, 50H, Ar-H), 7.36 (s, 108, Ar-H) ppm.

2.5.2. ATRP of DABSA Derivatives

The general procedure for atom transfer radical polymerization (ATRP) will be illustrated using DABSA and tris[2-(dimethylamino)ethyl]amine (Me_6TREN) as the ligand.

To a 25 mL Schlenk tube under a nitrogen atmosphere was added DABSA (0.712 gm, 3.00 mmol), and CuBr (4.30 mg, 0.0300 mmol, 1%), ethyl-2-bromopropionate (EBrP, 5.43 mg, 0.0300 mmol, 1%), and Me_6TREN (5.96 μL , 0.0300 mmol, 1%) in 2.00 mL of dry xylenes. After sparging the solution with nitrogen for 30 minutes, the flask

was lowered into an oil bath heated to 100 °C, and allowed to react for 48 hours. Analysis via ¹H NMR spectroscopy indicated no conversion to polymer.

2.5.3. ICAR ATRP of DABSA Derivatives

The general procedure for initiators for constant activator regeneration (ICAR) ATRP will be illustrated using DABSA, Me₆TREN as the ligand, and AIBN as the source of radicals that react with the transition metal complex to continuously regenerate its lower oxidative state.

To a 25 mL Schlenk tube under a nitrogen atmosphere was added DABSA (0.712 g, 3.00 mmol), and CuBr₂ (0.0340 mg, 1.50x10⁻⁴ mmol, 0.005%), EBrP (2.72 mg, 0.0150 mmol, 1%), and Me₆TREN (0.0298 μL, 1.50x10⁻⁴ mmol, 0.005%) in 2.00 mL of dry xylenes. After sparging the solution with nitrogen for 30 minutes, the flask was lowered into an oil bath heated to 100 °C, and allowed to react for 48 hours. Analysis via ¹H NMR spectroscopy indicated no conversion to polymer.

2.5.4. Reversible Addition-Fragmentation Chain Transfer (RAFT) Polymerization of DABSA-2,4-DF

To a 25 mL Schlenk tube under a nitrogen atmosphere was added DABSA-2,4-DF (0.728 g, 2.67 mmol), cyanomethyl methyl(phenyl) carbamodithioate (CMMPCDT, 29.59 mg, 0.133 mmol, 5%) and AIBN (21.88 mg, 0.133 mmol, 5%) in 1mL of dry xylenes. After sparging the solution with nitrogen for 30 minutes, the flask was lowered into an oil bath heated to 80 °C for 7 days, after which point the polymer was precipitated from diethyl ether to afford 0.085 g (12%) of **p2d** as a yellow solid.

2.6. ADMET Polymerization of DABSA Derivatives

The general procedure of acyclic diene metathesis (ADMET) polymerization will be illustrated using DABSA.

To a solution of DABSA (0.133 g, 0.56 mmol) in 0.56 mL of xylenes, was added Hoveyda-Grubbs 2nd Generation catalyst (11.4 mg, 0.0182 mmol, 3.25%). The solution was sparged with nitrogen for 25 minutes, then lowered into an oil bath heated to 70 °C and allowed to react under vacuum for 24 hours. The polymer was precipitated from diethyl ether and dried under vacuum to afford 0.069 g (52%) of **p3a** as a grey solid. The polymer was characterized by ¹H-NMR spectroscopy, GPC analysis, TGA, and DSC ($M_n = 14,915$ g/mol, $T_m = 115$ °C, $T_{d-5\%} = 146$ °C), ¹H NMR (CDCl₃, δ): 4.15 (s, 4H, N-CH₂), 5.67 (s, 2H, -CH=), 7.58 (m, 3H, Ar-H), 7.86 (m, 2H, Ar-H) ppm; ¹³C NMR (CDCl₃, δ): 54.9 (s, N-CH₂), 125.4 (s, -CH=), 127.3 (s, Ar-H), 129.1 (s, Ar-H), 132.7 (s, Ar-H), 137.3 (s, Ar-H) ppm.

The ADMET Polymerization of the remaining DABSA derivatives was carried out in an analogous fashion.

p3b (54%): $M_n = 8,690$ g/mol, $T_m = 136$ °C, $T_{d-5\%} = 167$ °C; ¹H-NMR (CDCl₃, δ): 4.14 (s, 4H, N-CH₂-), 5.69 (s, 2H, -CH=), 7.70 (m, 4H, Ar-H) ppm. ¹³C NMR (CDCl₃, δ): 54.9 (s, N-CH₂-), 125.4 (s, -CH=), 127.7 (s, Ar-Br), 128.8 (s, Ar-H), 132.4 (s, Ar-H), 136.4 (s, Ar-SO₂-) ppm.

p3c (50%): $M_n = 17,075$ g/mol $T_m = 90$ °C, $T_{d-5\%} = 159$ °C; ¹H-NMR (CDCl₃, δ): 4.13 (s, 4H, N-CH₂-), 5.68 (s, 2H, -CH=), 7.22 (t, 2H, Ar-H), 7.86 (m, 2H, Ar-H) ppm. ¹³C (CDCl₃, δ): 54.9 (s, N-CH₂-), 116.4 (d, Ar-H), 125.4 (s, -CH=), 130.0 (d, Ar-H), 133.5 (s, Ar-SO₂), 165.1 (d, Ar-F) ppm.

p3d (49%): $M_n = 5,550$ g/mol $T_m = 65.5$ °C, $T_{d-5\%} = 146$ °C; $^1\text{H-NMR}$ (CDCl_3 , δ): 4.24 (s, 4H, N-CH₂-), 5.75 (s, 2H, -CH=), 6.99 (m, 3H, Ar-H), 7.96 (m, 1H, Ar-H) ppm. ^{13}C (CDCl_3 , δ): 54.5 (s, N-CH₂-), 105.7 (t, Ar-H), 111.7 (dd, Ar-H), 122.9 (m, Ar-SO₂), 125.4 (s, -CH=), 132.9 (dd, Ar-H), 159.7 (dd, Ar-F), 165.6 (dd, Ar-F).

p3e (58%): $M_n = 10,210$ g/mol, $T_m = 109$ °C, $T_{d-5\%} = 125$ °C; $^1\text{H-NMR}$ (CDCl_3 , δ): 4.17 (s, 4H, N-CH₂), 5.72 (s, 2H, -CH=), 7.06 (tt, 1H, Ar-H), 7.39 (m, 2H, Ar-H) ppm; ^{13}C (CDCl_3 , δ): 55.0 (s, N-CH₂-), 108.3 (t, Ar-H), 110.7 (dd, Ar-H), 125.4 (s, -CH=), 140.7 (t, Ar-SO₂-), 162.9 (dd, Ar-F) ppm.

2.7. S_NAr Copolymerization of **2a/b** and **1d/e** using 4,4'-dihydroxydiphenyl ether

The general procedure for nucleophilic aromatic substitution (S_NAr) copolymerization will be illustrated using 2,4-DFDOctBSA (**2a**), and DABSA-2,4-DF (**1d**).

To a solution of **2a** (0.595 g, 1.43 mmol, 95%), **1d** (0.0205 g, 0.0750 mmol, 5%), and 4,4'-dihydroxydiphenyl ether (0.303 g, 1.5 mmol) in 4.69 mL of NMP, was added K₂CO₃ (0.311 g, 2.25 mmol) and the solution sparged for 25 minutes then lowered into an oil bath heated to 135 °C and allowed to react for 72 hours. The polymer was precipitated from water and dried under vacuum to afford 0.492 g (58.6%) of 95/5-poly(2,4-DOctBSA-co-2,4-DABSA) (**p4a**, $M_n = 3,660$ g/mol, $T_g = 14.5$ °C, $T_{d-5\%} = 354$ °C), $^1\text{H-NMR}$ (CDCl_3 , δ): 0.87 (m, 6H, -CH₃), 1.24 (s, 20H, -CH₂-), 1.53 (m, 4H, -CH₂-), 3.27 (m, 4H, N-CH₂-), 3.96 (m, 4H, N-CH₂-), 5.17 (d, m, 4H, =CH₂), 5.69, (m, 2H, -CH=), 6.54 (m, 2H, Ar-H), 7.02 (m, 4H, Ar-H), 7.28 (s, 2H, Ar-H), 7.92 (d, 2H, Ar-H) ppm; DEPT 90 ^{13}C NMR (CDCl_3 , δ): 107.0 (s, Ar-H), 109.5 (s, Ar-H), 120.2 (s, Ar-H), 121.6 (d, Ar-H), 132.9 (s, -CH=) ppm.

S_NAr copolymerization of **1e/2b** was carried out in an analogous fashion.

p4b (54.3%): $M_n = 3,050$ g/mol; $T_g = 6.34$ °C; $T_{d-5\%} = 329$ °C; 1H NMR ($CDCl_3$, δ): 0.89 (m, 6H, $-CH_3$), 1.27 (s, 20H, $-CH_2-$), 1.52 (m, 4H, $-CH_2-$), 3.15 (m, 4H, N- CH_2-), 3.79 (m, 4H, N- CH_2-), 5.16 (m, 4H, $=CH_2$), 5.64 (m, 2H, $-CH=$), 6.79 (m, 2H, Ar-H), 7.11 (m, 4H, Ar-H), 7.37 (d, 4H, Ar-H) ppm; DEPT 90 ^{13}C NMR ($CDCl_3$, δ): 110.0 (s, Ar-H), 110.7 (s, Ar-H), 121.4 (s, Ar-H), 136.0 (s, $-CH=$) ppm.

2.8. Characterization

2.8.1. Size Exclusion Chromatography (SEC)

Size exclusion chromatography (SEC) was used to determine molecular weight and molecular weight distributions of polymers in THF/5% acetic acid. Number average molecular weights (M_n) and dispersity (D) were determined using the refractive index (RI) signal, the weight average molecular weight (M_w) were determined via the light scattering signal. Calibration was done using polystyrene standards.

2.8.2. Differential Scanning Calorimetry (DSC)

The thermal transition temperatures of the materials were determined using a TA Instruments Q200 Differential Scanning Calorimeter. The melting point of the monomers were determined by heating 5 mg of sample, in a T_{zero} aluminum pan, at 10 °C/min from -185 to 50 °C. A typical method of determining the thermal transition temperatures of polymers included heating 5 mg of sample, in a T_{zero} aluminum pan, at 10 °C/min from 40 to 150 °C and cooling at 10 °C/min to 0 °C in two cycles under a nitrogen atmosphere. The glass transition temperature (T_g) was determined at the midpoint of the tangent of the second heating cycle. The first heating cycle was utilized to erase the thermal history of

the polymers, and the melting temperature (T_m) was determined at the endothermic peak of the second heating cycle.

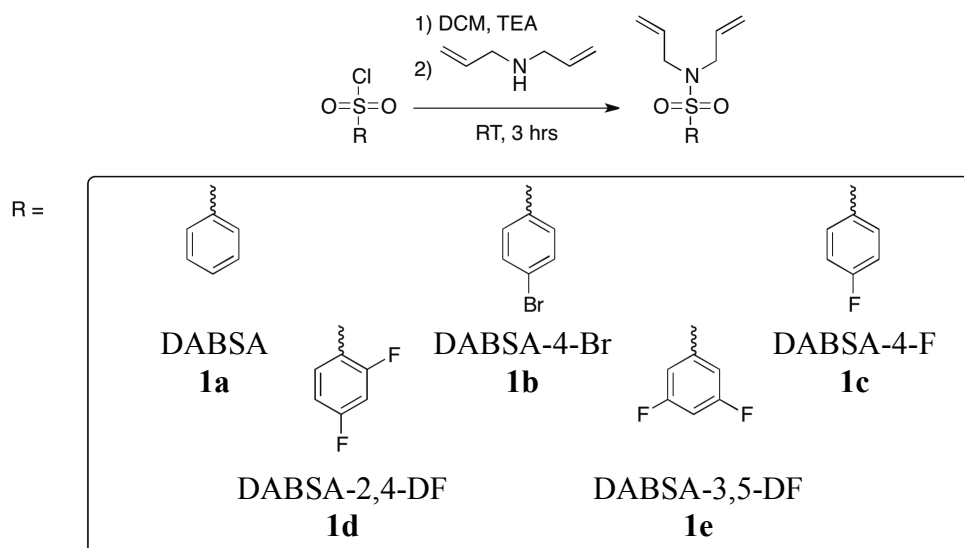
2.8.3. Thermogravimetric Analysis (TGA)

The thermal stability of the polymers was investigated using a TA Instruments Q500 Thermogravimetric Analyzer. The analysis involved heating a sample of 5 mg at a rate of 10 °C/min from 40 to 800 °C under a nitrogen atmosphere. The weight loss was recorded as a function of temperature, and the thermal stability was reported as 5% weight loss ($T_{d-5\%}$).

3. RESULTS AND DISCUSSION

3.1. Monomer Synthesis

A series of bifunctional monomers based on *N,N*-diallylbenzenesulfonamide (DABSA) with varying groups present on the benzene moiety, was investigated. Using the appropriate benzenesulfonyl chloride (BSC) derivative as a starting material, five monomers were prepared via nucleophilic substitution, as shown in **Scheme 15**. For each of the reactions, commercially available triethyl amine (TEA) and diallylamine were allowed to react with the BSC derivative in DCM for approximately three hours, at which point GC/MS analysis indicated complete conversion of the starting materials to the desired product.



Scheme 15. Synthetic route for DABSA derivatives.

3.1.1. Synthesis of *N,N*-diallylbenzenesulfonamide (DABSA) Derivatives

Using benzenesulfonyl chloride as a starting material, *N,N*-diallylbenzenesulfonamide (DABSA), **1a**, was prepared by nucleophilic substitution. Commercially available benzenesulfonyl chloride was allowed to react at room temperature with triethyl amine for fifteen minutes, at which point diallylamine was added and allowed to react for 3 hours, during which time an exothermic reaction occurred. GC/MS analysis of an aliquot confirmed that the starting materials were converted to the desired product. After washing with HCl/water, and removing the DCM via rotary evaporation, the product was isolated to afford **1a** as a yellow oil in a 90 % yield.

The structure was confirmed by ^1H and ^{13}C NMR spectroscopy, GC/MS, and elemental analysis. The ^1H and ^{13}C NMR spectra of **1a** are presented in **Figure 4** and **Figure 6**, respectively. Integration of the ^1H NMR spectrum confirmed the correct number of hydrogens in the monomer. There are six unique peaks that appear in the ^1H NMR spectrum of **1a** (**Figure 4**). The most upfield proton **c** appears as a doublet at 3.84 ppm ($^3J_{\text{H-H}} = 6.28$ Hz) due to coupling with an adjacent hydrogen atom. Both the *cis*- (**a'**) and *trans*- (**a**) protons appear as multiplets from 5.12-5.15 and 5.17-5.19 ppm, respectively. Protons **a** and **a'** can be distinguished by the difference in shielding; **a'** is more shielded by the CH_2 than is **a**, resulting in **a'** being more upfield. Protons **b** and **d** appear as a series of multiplets from 5.55-5.69 and from 7.83-7.87 ppm, respectively. Protons **e** and **f** appear as a complex series of overlapping multiplets from 7.49-7.62 ppm.

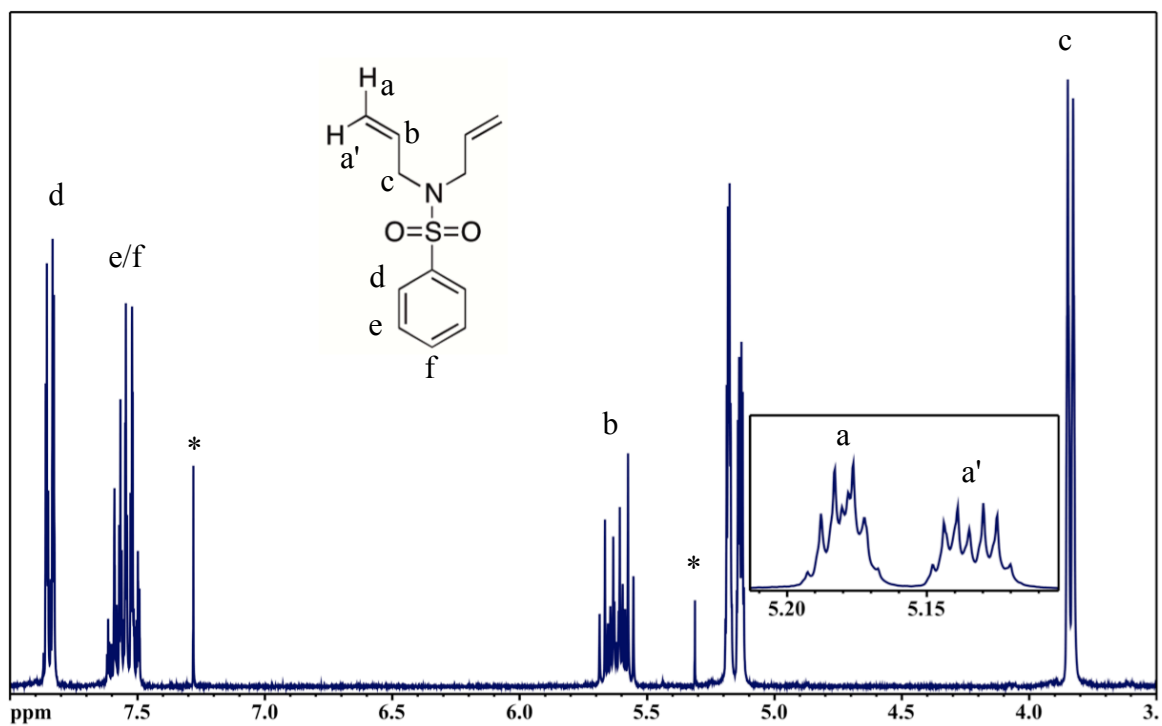


Figure 4. 300 MHz ^1H NMR spectrum (CDCl_3) of **1a**.

Syntheses of the remaining *N,N*-diallylbenzenesulfonamide derivatives were carried out in an analogous fashion, and the major differences between the ^1H and ^{13}C NMR spectra are the specific signals in the aromatic region, arising from the benzenesulfonyl chloride derivative used for the synthesis (see **Figure 5** and **Figure 7**). Protons **a-c** and carbons **a-c** appear in essentially the same positions in monomers **1a-e**.

N,N-diallyl-4-bromobenzenesulfonamide (**1b**) was prepared in a 96% yield as a yellow oil, and in the ^1H NMR spectrum protons **d** and **e** appear as a series of broad, overlapping multiplets from 7.58-7.69 ppm. *N,N*-diallyl-4-fluorobenzenesulfonamide (**1c**) was prepared in a 86% yield as a yellow oil; protons **d** and **e** appear as a series of broad multiplets from 7.78-7.85 and 7.13-7.19 ppm, respectively. *N,N*-diallyl-2,4-difluorobenzenesulfonamide (**1d**) was prepared in a 94% yield as a yellow oil; proton **d** appears as a multiplet from 7.86-7.95 ppm, and protons **e** and **f** appear as a series of broad, overlapping multiplets from 6.89-7.01 ppm. *N,N*-diallyl-3,5-

difluorobenzenesulfonamide (**1e**) was prepared in a 93% yield as a white powder; proton **d** appears as a series of broad multiplets from 7.33-7.42 ppm respectively, while proton **e** appears as a triplet of triplets at 7.03 ppm due to coupling with two *ortho*-fluorines with equal coupling constants ($^3J_{\text{H-F}} = 8.47$ Hz) and two *meta*-hydrogens with equal coupling constants ($^4J_{\text{H-H}} = 2.32$ Hz).

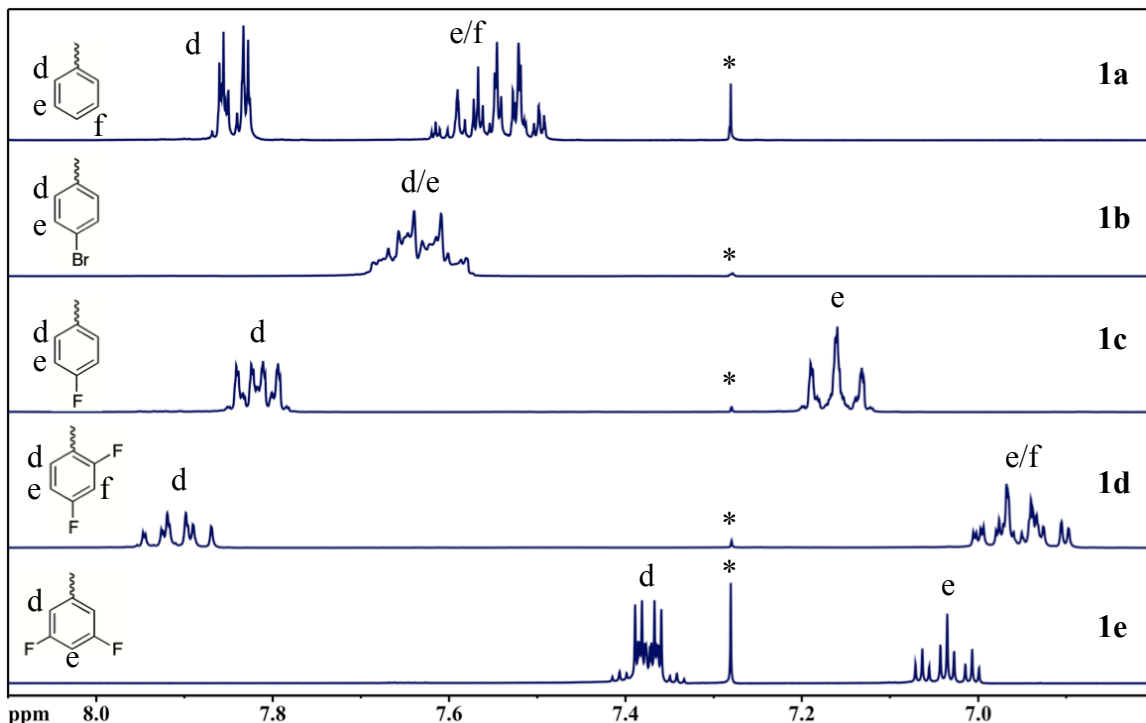


Figure 5. 300 MHz NMR spectra (CDCl_3) of the aromatic region of **1a-e**.

In the ^{13}C NMR spectrum of **1a** (**Figure 6**), carbons **a**, **b**, **c**, **d**, **e**, **f**, and **g** appear as singlets at 119.0, 132.5, 49.3, 140.4, 127.1, 129.1, and 132.5 ppm, respectively. Carbons **b** and **g** appear at 132.5 ppm, and the two peaks can be distinguished by the shielding associated with **g**. Carbon **g** experiences a greater pull of electrons from the *para*-sulfone than carbon **b** does from the *ipso*- $\text{CH}_2\text{-N}$, resulting in **g** being slightly more upfield.

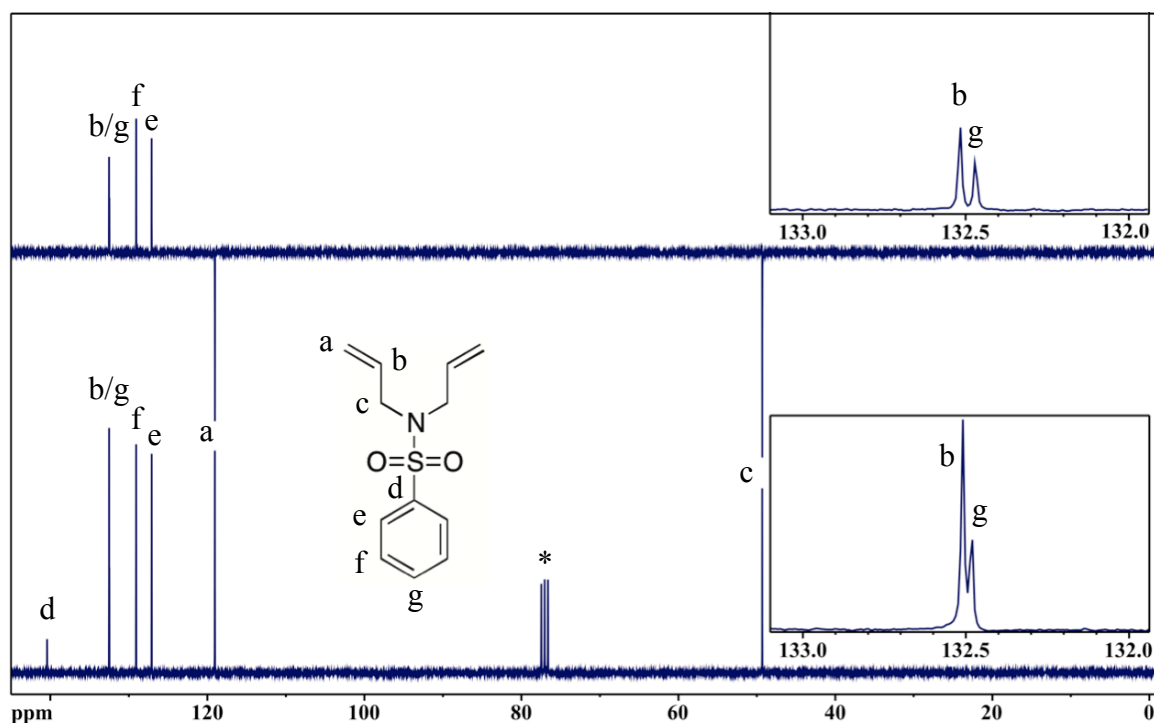


Figure 6. 75.7 MHz DEPT 135 (top) and ^{13}C NMR (bottom) spectral overlay (CDCl_3) of DABSA.

The ^{13}C NMR spectra of **1a-1e** are presented in **Figure 7**. In the ^{13}C NMR spectrum of **1b**, carbons **d**, **e**, and **g** appear as singlets at 139.5, 128.7, and 127.3 ppm, respectively. Both carbons **b** and **f** appear at 132.3 ppm, and the two peaks can be distinguished by the shielding associated with **f**. Carbon **f** experiences a greater pull of electrons from the *para*-sulfone than carbon **b** does from the *ipso*- $\text{CH}_2\text{-N}$, resulting in **f** being slightly more upfield. In the ^{13}C NMR spectrum of **1c**, carbons **d** at 136.4 ($^4J_{\text{C-F}} = 3.29$ Hz), **e** at 129.8 ppm ($^3J_{\text{C-F}} = 9.30$ Hz), **f** at 116.1 ppm ($^2J_{\text{C-F}} = 22.5$ Hz), and **g** at 166.4 ppm ($^1J_{\text{C-F}} = 254$ Hz) all appear as doublets. In the ^{13}C NMR spectrum of **1d**, carbon **d** appears as a multiplet from 125.2-125.6 ppm, carbon **h** appears as a triplet at 105.6 ppm ($^2J_{\text{C-F}} = 25.7$ Hz) due to splitting with two ortho fluorines. Carbon **f** appears as a doublet of doublets at 111.6 ppm ($^2J_{\text{C-F}} = 3.81$ Hz, $^4J_{\text{C-F}} = 21.6$ Hz) due to splitting with *ortho*- and *para*-fluorines. Carbon **e** appears as a doublet of doublets at 132.5 ppm ($^3J_{\text{C-F}}$

= 2.2 Hz, ${}^3J_{C-F}$ = 10.2 Hz) due to splitting with two non-equivalent *meta*-fluorines. Carbons **g** at 165.6 ppm (${}^1J_{C-F}$ = 13.5 Hz, ${}^3J_{C-F}$ = 259 Hz) and **i** at 159.5 ppm (${}^1J_{C-F}$ = 14.4 Hz, ${}^3J_{C-F}$ = 260 Hz) both appear as doublets of doublets due to coupling with two non-equivalent fluorine atoms. In the ${}^{13}\text{C}$ NMR spectrum of **1e**, carbons **d** 143.9 ppm (${}^3J_{C-F}$ = 8.15 Hz), and **g** at 108.0 ppm (${}^2J_{C-F}$ = 25.1 Hz) both appear as triplets at due to splitting with two equivalent fluorine atoms. Carbons **e** at 110.6 ppm (${}^2J_{C-F}$ = 9.39 Hz, ${}^4J_{C-F}$ = 18.3 Hz) and **f** at 162.8 ppm (${}^1J_{C-F}$ = 11.6 Hz, ${}^3J_{C-F}$ = 255 Hz) both appear as a doublet of doublets due to splitting with two non-equivalent fluorine atoms.

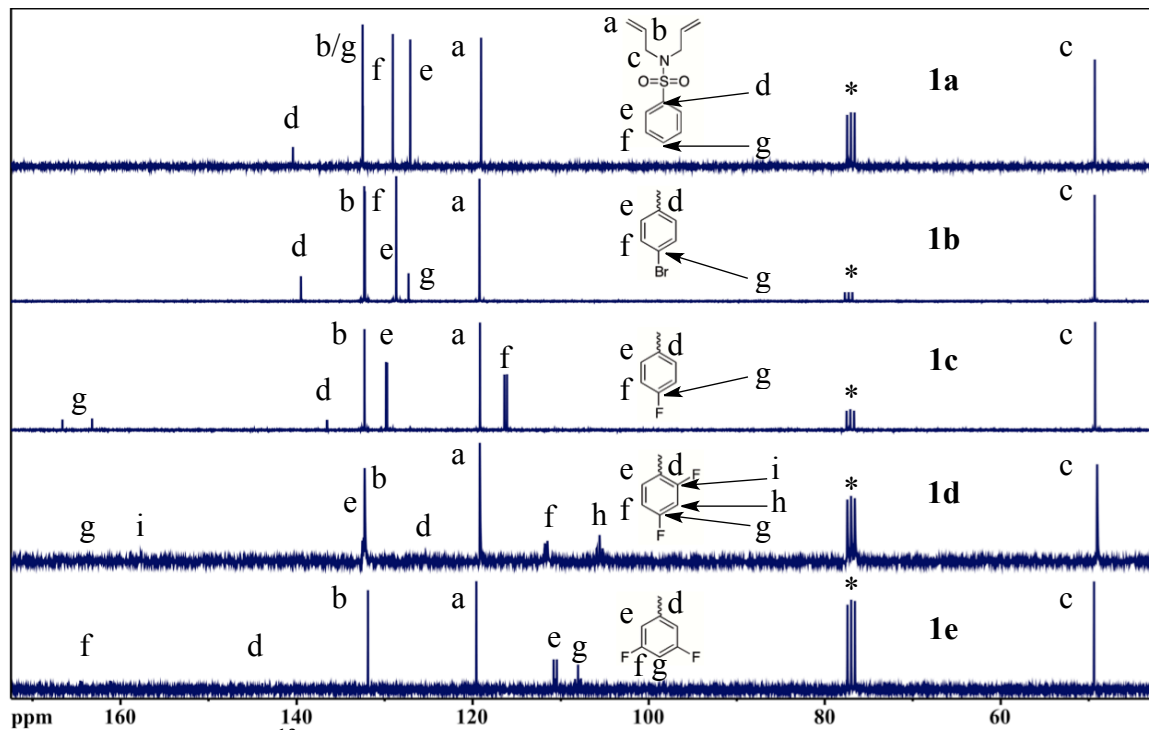
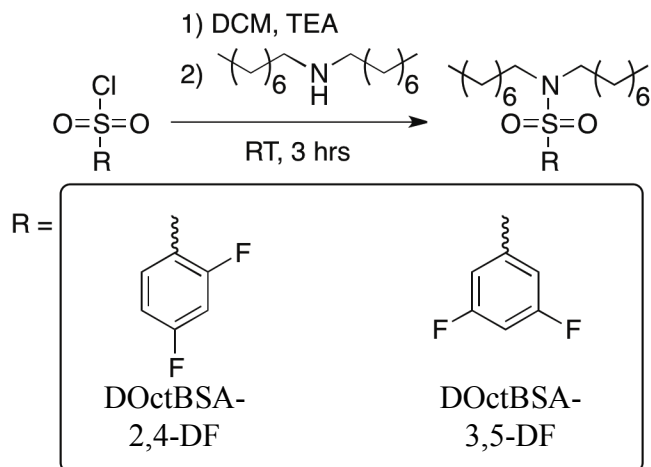


Figure 7. 75.5 MHz ${}^{13}\text{C}$ NMR spectral overlay (CDCl_3) of DABSA derivatives.

3.1.2. Synthesis of *N,N*-dioctylbenzenesulfonamide Derivatives

Using 2,4-difluorobenzenesulfonyl chloride as a starting material, *N,N*-dioctyl-2,4-difluorobenzenesulfonamide (DOctBSA-2,4-DF, **2a**) was prepared by nucleophilic substitution, as illustrated in **Scheme 16**. Commercially available 2,4-difluorobenzenesulfonyl chloride was allowed to react at room temperature with triethyl

amine (TEA) for fifteen minutes, at which point dioctylamine was added and allowed to react for 3 hours, during which time an exothermic reaction occurred. GC/MS analysis of an aliquot confirmed that the starting materials had been converted to the desired product. After washing with HCl/water, hexanes, and removing the DCM via rotary evaporation, the product was isolated to afford **2a** as a yellow oil in a 86 % yield.



Scheme 16. Synthetic route for DOctBSA derivatives.

The structure was confirmed by ^1H , DEPT 135, and ^{13}C NMR spectroscopy, GC/MS, and elemental analysis. Integration of the ^1H NMR spectrum confirmed the structure of the monomer. The ^1H NMR spectrum (**Figure 8**) contains six unique peaks. The most upfield proton, **a**, appears as a triplet at 0.89 ppm ($^3J_{\text{H-H}} = 6.81$ Hz) due to coupling with two adjacent hydrogens with equivalent coupling constants. Protons **c-g** appear as a broad multiplet from 1.22-1.33 ppm due to coupling with adjacent hydrogens. Protons **b** and **i** appear as broad multiplets from 1.45-1.58 ppm and 7.89-7.97 ppm, respectively. Protons **i** and **j** appear as a series of broad, overlapping multiplets from 6.90-7.02 ppm.

Synthesis of *N,N*-dioctyl-3,5-difluorobenzenesulfonamide (DOctBSA-3,5-DF, **2b**) was carried out in an analogous fashion, and the major differences between the ^1H and

^{13}C NMR spectra are the specific signals in the aromatic region, arising from the monomer used. Protons **a-h** and carbons **a-h** appear in essentially the same positions in both of the monomers.

Monomer **2b** was prepared in a 76% yield as a yellow oil; proton **i** appears as a multiplet from 7.33-7.38 ppm, and proton **j** appears as a triplet of triplets at 7.01 ppm due to coupling with two *ortho*-fluorines with equal coupling constants ($^3J_{\text{H-F}} = 8.50$ Hz) and two *meta*-hydrogens with equal coupling constants ($^4J_{\text{H-H}} = 2.31$ Hz)

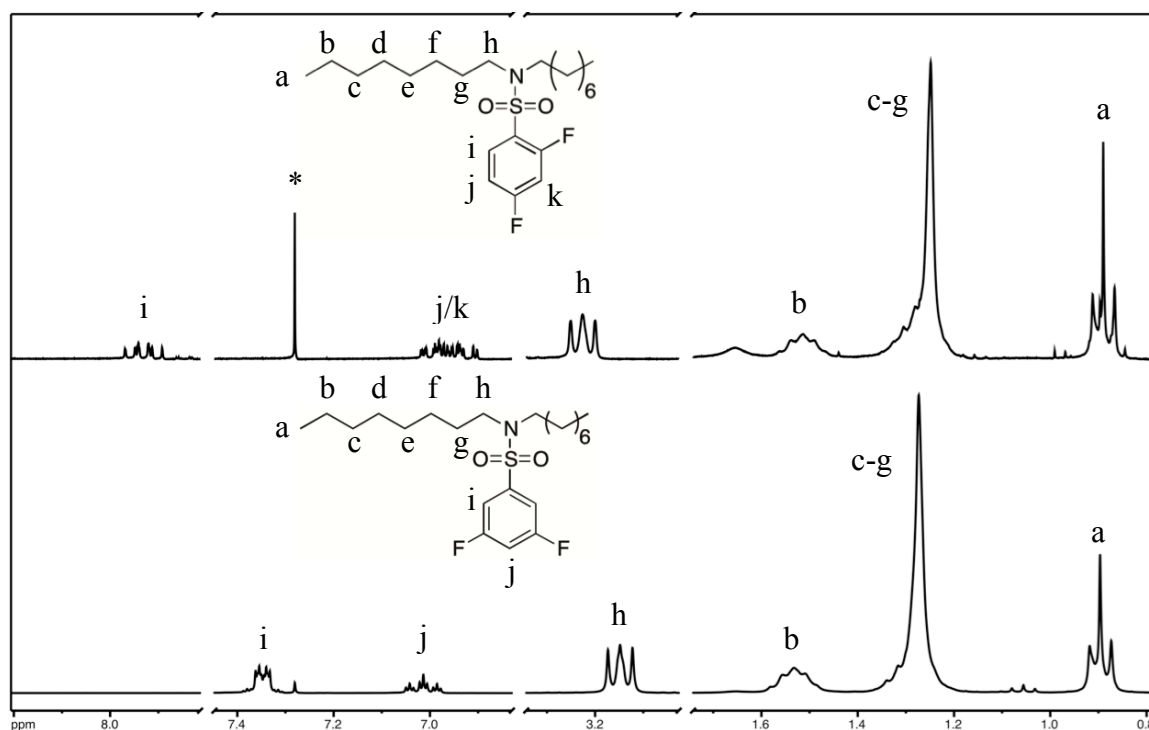


Figure 8. ^1H NMR spectral overlay (CDCl_3) of **2a** (top) and **2b** (bottom).

The DEPT 135 and ^{13}C NMR spectra of **2a** (**Figure 9**) contain 10 and 14 peaks, respectively. Carbons **a** at 13.9 ppm, **b** at 22.5 ppm, **g** at 26.5 ppm, **f** at 28.4 ppm, and **c** at 31.7 ppm appear as singlets. Protons **d** and **e** appear as singlets at 29.1 ppm, with proton **e** shifted slightly more upfield due to shielding from the nitrogen. Carbon **h** appears as a doublet at 47.5 ppm ($J_{\text{C,F}} = 2.27$ Hz) due to through-space coupling with the fluorine *ortho*- to the sulfonamide. Carbon **m** appears as a triplet at 105.3 ppm ($^2J_{\text{C-F}} = 25.8$) due

to coupling with two similar fluorine atoms. Carbons **k** at 111.4 ppm ($^2J_{C-F} = 3.74$ Hz, $^4J_{C-F} = 21.6$ Hz), **i** at 125.3 ppm ($^2J_{C-F} = 3.90$ Hz, $^4J_{C-F} = 15.2$ Hz), **j** at 132.4 ppm ($^3J_{C-F} = 2.29$ Hz, $^3J_{C-F} = 10.2$ Hz), **n** at 159.4 ppm ($^1J_{C-F} = 12.5$ Hz, $^3J_{C-F} = 257$ Hz), and **l** at 165.3 ppm ($^1J_{C-F} = 11.3$ Hz, $^3J_{C-F} = 256$ Hz) each appear as a doublet of doublets due to coupling with two non-equivalent fluorine atoms.

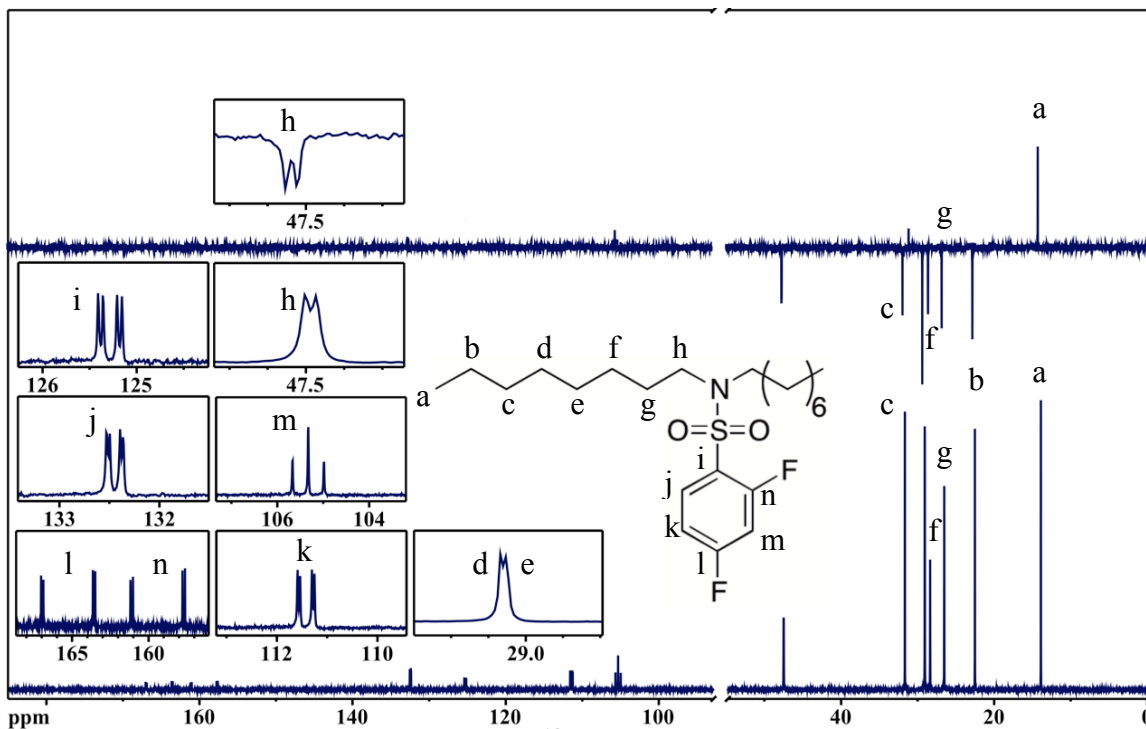


Figure 9. 75.5 MHz DEPT 135 (top) and ^{13}C (bottom) NMR spectral overlay (CDCl_3) of **2a**.

The DEPT 135 and ^{13}C NMR spectra of **2b** (Figure 10) contain nine and twelve unique peaks, respectively. Carbons **a** at 14.0 ppm, **b** at 22.6 ppm, **c** at 31.7 ppm, **d** and **e** at 29.1 ppm, **f** at 28.6 ppm, **g** at 26.7 ppm, and **h** at 48.2 ppm appear as singlets. Carbons **i** at 143.7 ppm ($^3J_{C-F} = 7.99$ Hz) and **l** at 107.7 ppm ($^2J_{C-F} = 25.1$ Hz) appear as triplets due to splitting with a *para*- and *ortho*- fluorine, respectively. Carbons **j** at 110.5 ppm ($^2J_{C-F} = 9.26$ Hz, $^4J_{C-F} = 18.2$ Hz) and **k** at 162.8 ppm ($^1J_{C-F} = 11.6$ Hz, $^3J_{C-F} = 254$ Hz) appear as doublets of doublets due to splitting with two non-equivalent fluorine atoms.

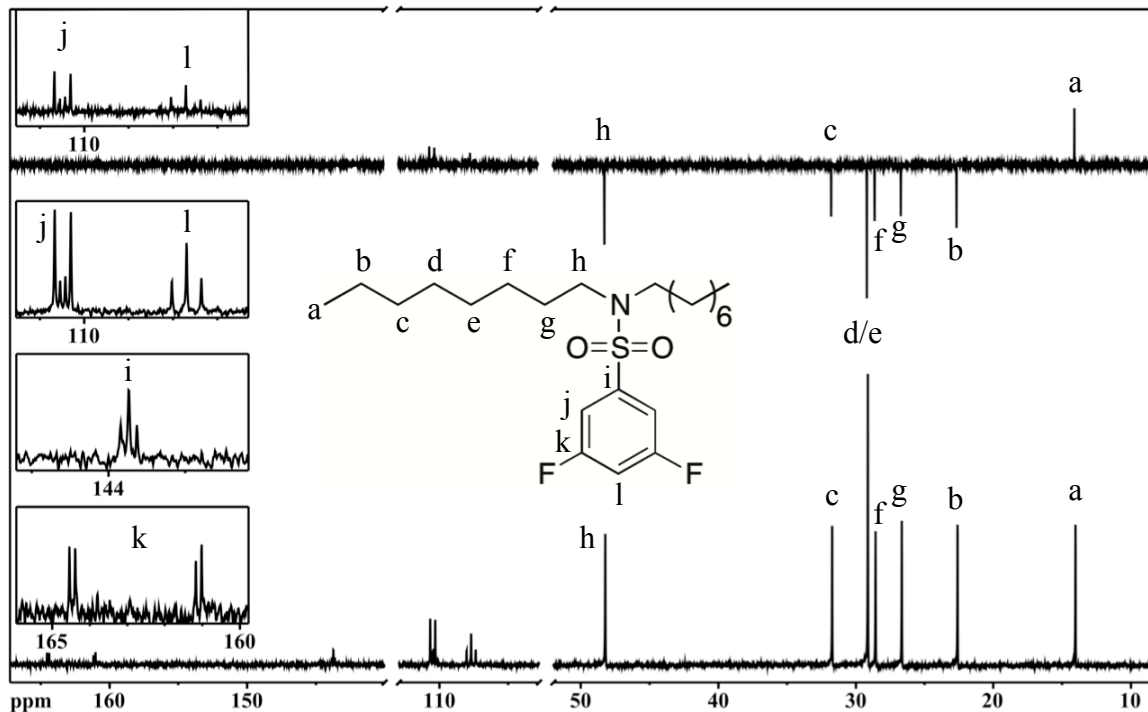


Figure 10. 75.5 MHz DEPT 135 (top) and ^{13}C NMR (bottom) spectral overlay (CDCl_3) of **2b**.

3.1.3. Spartan Calculations

The energy of monomers **1a-e** was calculated in vacuum using the Spartan' 10 computational software package (Wavefunction, Inc., Irvin, CA). The geometries were initially optimized using the semiempirical method RM1, and then further optimized using density functional theory at the B3LYP/6-31+G** level. The energy of each of the monomers was recorded and expressed as a relative energy with respect to the most stable species of that charge. As shown in **Table 2**, by incorporating the benzenesulfonamide moiety, the electrostatic charge on the nitrogen becomes significantly more positive; which, as previously stated, reduces the rate of degradative chain transfer, and indicates that a higher molecular weight polymer can be formed.

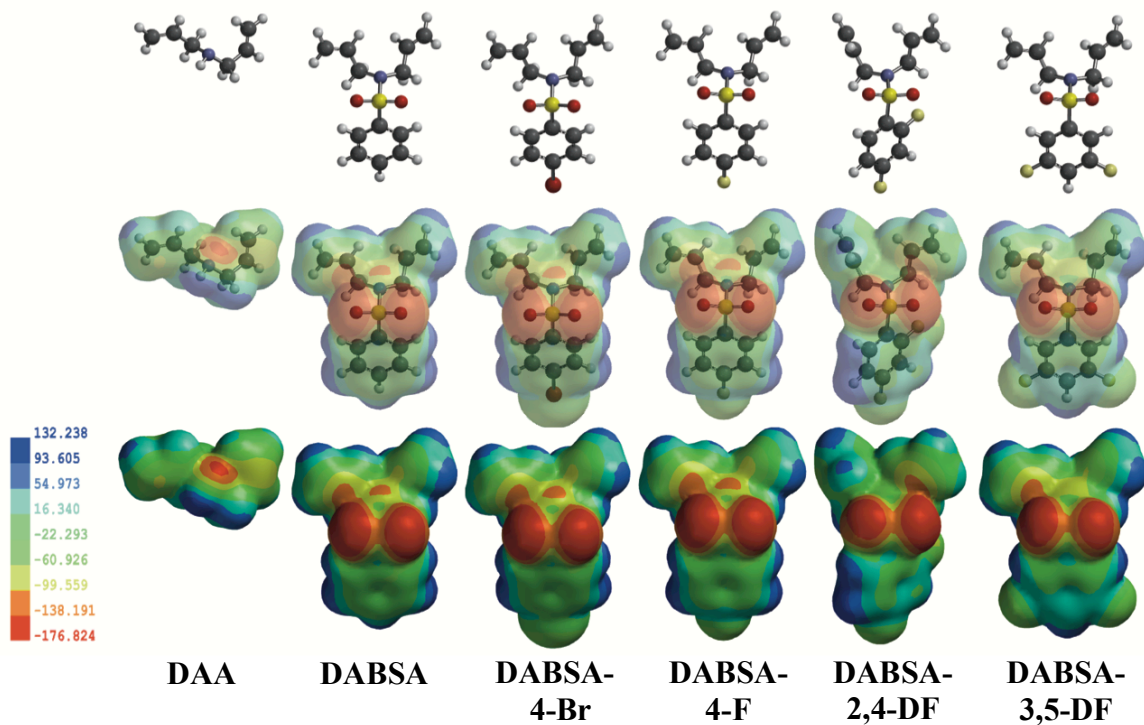


Figure 11. Electron density mapping of starting materials.

Table 2. Calculated electrostatic charges of diallylamine derivatives.

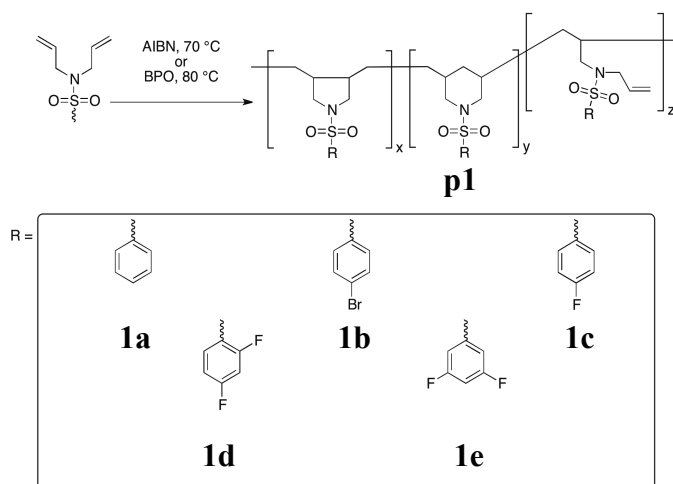
Compound	Electrostatic Charge on Nitrogen Atom
Diallylamine	-0.641
DABSA (1a)	-0.105
DABSA-4-Br (1b)	-0.138
DABSA-4-F (1c)	-0.131
DABSA-2,4-DF (1d)	-0.134
DABSA-3,5-DF (1e)	-0.139

The most negative charge on the nitrogen was on diallylamine, while the most positive charge on the nitrogen atom was calculated on DABSA. The monomers containing halides (**1b-e**) have a slightly more negative charge than does DABSA, which

can be explained through electron donating effects. Both fluorine and bromine withdraw electron density through inductive effects, but strongly donate *ortho*- and *para*- through resonance effects. The *meta*-fluorines in DABSA-3,5-DF are electron withdrawing through inductive effects on the carbon *ipso*- to the sulfonamide, resulting in a decrease in electron density at that position. However, the contribution through resonance is much greater than the inductive effects, the two fluorine groups donate electron density to the *ortho*- and *para*- positions through resonance, resulting in a benzene ring that is more electron rich than it is in monomers **1a-d**. As shown in **Table 3**, these calculations also correlate with the difference in chemical shift of the allyl groups in the ^{13}C NMR spectra of the monomers.

3.1.4. Free Radical Polymers

Polymers **p1a-e** were prepared via the free radical polymerization (FRP) of monomers **1a-e**, as outlined in **Scheme 17**. For each of the reactions, commercially available 2,2'-azobis(2-methylpropionitrile) (AIBN) or benzoyl peroxide (BPO) was allowed to react with the DABSA derivative for approximately twenty-four hours. AIBN was selected as the initiator for FRP because the resulting polymers typically had a higher yield and greater thermal stability than those prepared with BPO, as shown in **Table 4**.



Scheme 17. General outline of the FRP of DABSA derivatives.

The polymers were precipitated from diethyl ether, centrifuged, washed again with diethyl ether, and isolated as off-white solids by the removal of diethyl ether by decantation and vacuum. The structures were confirmed by ^1H NMR Spectroscopy, SEC, TGA, and DSC, while the cyclization efficiencies (CE) were determined by integrating the double bond proton peaks relative to the backbone proton peaks in the ^1H NMR spectrum (**Figure 12**).

3.1.4.1 AIBN Initiated Polymerization of DABSA Derivatives

AIBN initiated **p1a** was prepared in a 51% yield, with a cyclization efficiency of 97.5%. Protons **a** and **b** appear as a series of broad multiplets from 5.12-5.18 ppm and 5.54-5.67 ppm, respectively (see **Figure 12**). Proton **c** appears as a doublet at 3.83 ppm ($^3J_{\text{H-H}} = 5.90$ Hz) due to coupling with an adjacent hydrogen atom. The decrease in intensity of protons **a-c** indicates successful polymerization of **1a**, while the residual allyl peaks indicated that 100% cyclization did not occur. Protons **n**, and **o/p** appear as broad singlets from 7.75-7.90 and 7.45-7.65 ppm, respectively, and protons **d-m** appear as a broad series of multiplets from 0.61-3.50 ppm, both of which are typical in FRP.

AIBN initiated FRP of the remaining *N,N*-diallylbenzenesulfonamide derivatives were carried out in an analogous fashion, and the major differences between the ^1H spectra (**Figure 12**) are the specific signals in the aromatic region, arising from monomer used, with protons **a-m** appear in essentially the same positions in each of the polymers.

AIBN initiated **p1b** was prepared in an 84% yield, with a cyclization efficiency of 98.2%; protons **n** and **o** appear as broad singlets from 7.63-7.78, which is typical in FRP. AIBN initiated **p1c** was prepared in a 63% yield, with a cyclization efficiency of 97.9%; protons **n** and **o** appear as broad singlets from 7.79-7.91 and 7.15-7.31 ppm, respectively, which is typical in FRP. AIBN initiated **p1d** was prepared in a 67% yield, with a cyclization efficiency of 99.3%; protons **n** and **o/p** appear as broad multiplets from 7.81-8.00 and 6.90-7.21 ppm, respectively, which is typical in FRP. AIBN initiated **p1e** was prepared in a 90% yield, with a cyclization efficiency of 98.8%; protons **n** and **o** appear as broad singlets from 7.25-7.47 and 6.96-7.22 ppm, respectively, which is typical in FRP.

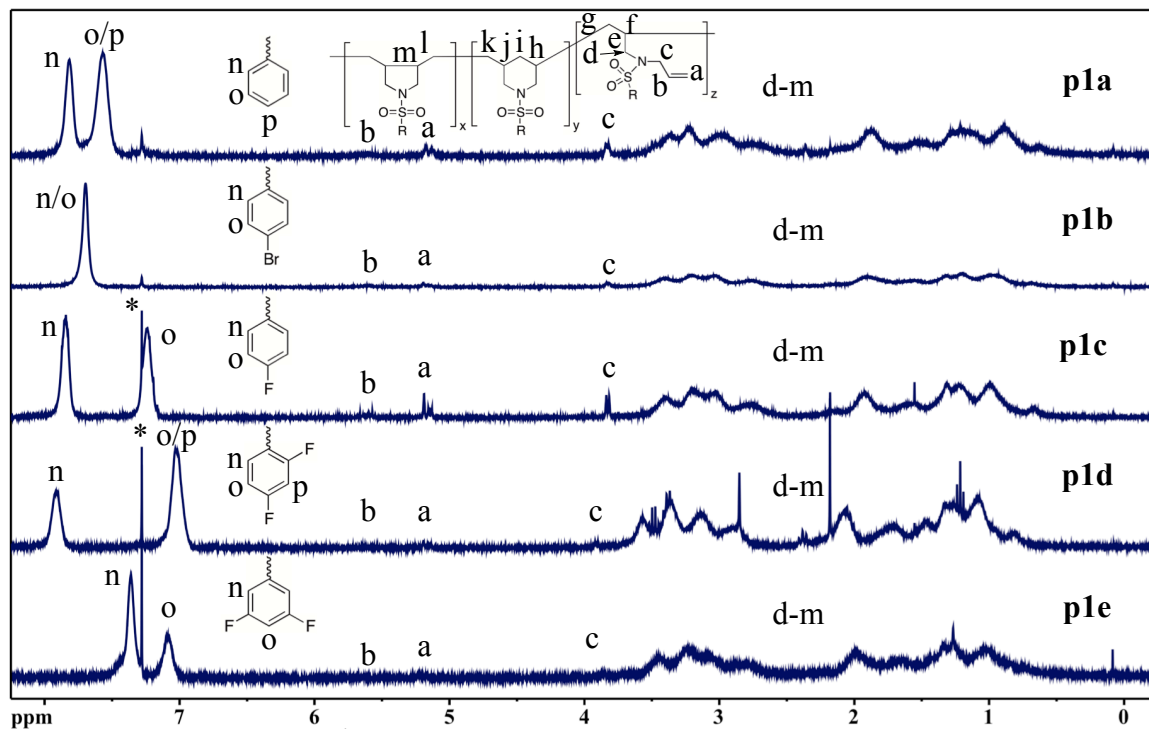


Figure 12. 300 MHz ^1H NMR spectral overlay (CDCl_3) of AIBN initiated **p1a-e**.

3.1.4.2 BPO Initiated Polymerization of DABSA Derivatives

Benzoyl peroxide (BPO) initiated **p1a** was prepared in a 49% yield, with a cyclization efficiency of 98.8%. Protons **a** and **b** appear as a series of broad multiplets from 5.14-5.20 ppm and 5.54-5.67 ppm, respectively (see **Figure 13**). Proton **c** appears as a doublet at 3.83 ppm ($^3J_{\text{H-H}} = 5.90$ ppm) due to coupling with an adjacent hydrogen. Protons **n** and **o/p** appear as broad singlets from 7.71-7.91 and 7.36-7.70 ppm, respectively, and protons **d-m** appear as a broad series of multiplets from 0.43-3.50 ppm, both of which are typical in FRP. The additional peaks present in the aromatic region are attributed to the phenyl ring in BPO.

BPO initiated FRP of the remaining *N,N*-diallylbenzenesulfonamide derivatives were carried out in an analogous fashion, and the major differences between the ^1H spectra (**Figure 13**) are the specific signals in the aromatic region, arising from monomer

used, with protons **a-m** appearing in essentially the same positions in each of the polymers.

BPO initiated **p1d** was prepared in a 58% yield, with a cyclization efficiency of 99.3%; protons **n** and **o/p** appear as broad singlets from 7.80-8.01 and 6.89-7.15 ppm, respectively, which is typical in FRP. BPO initiated **p1e** was prepared in a 56% yield, with a cyclization efficiency of 98.8%; protons **n** and **o** appear as broad singlets from 7.25-7.52 and 6.69-7.19 ppm, respectively, which is typical in FRP.

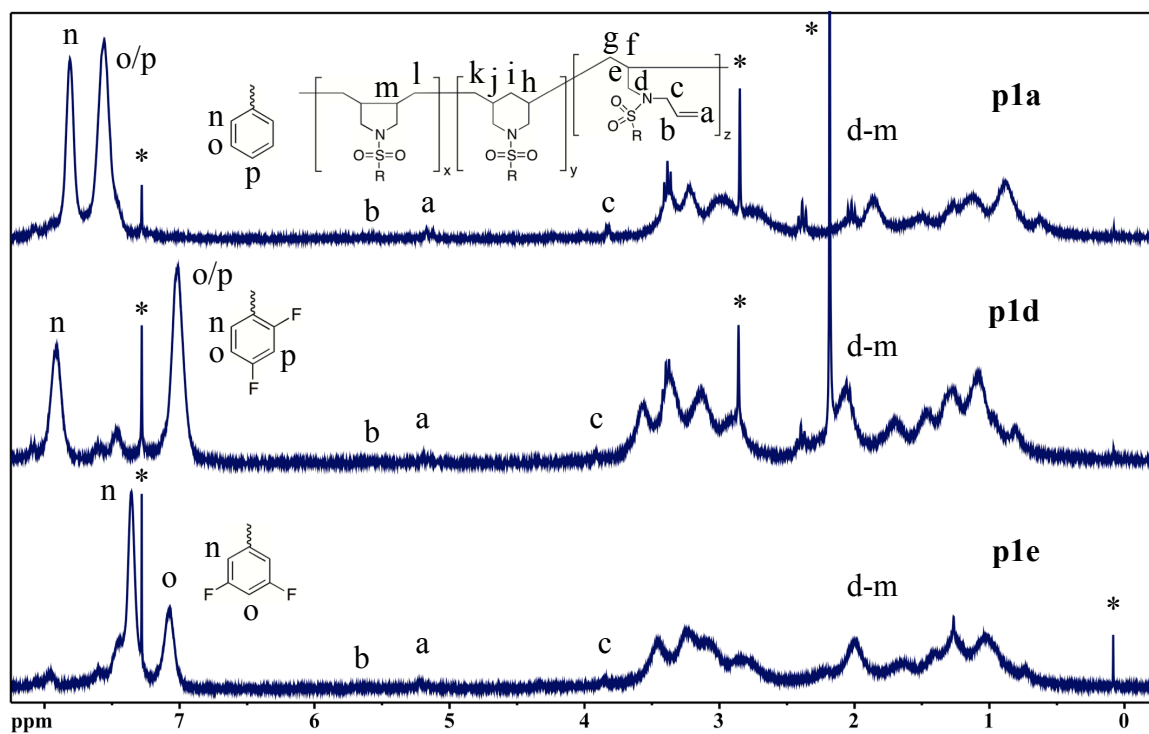


Figure 13. 300 MHz ^1H NMR spectral overlay (CDCl_3) of BPO initiated **p1a**, **d**, and **e**.

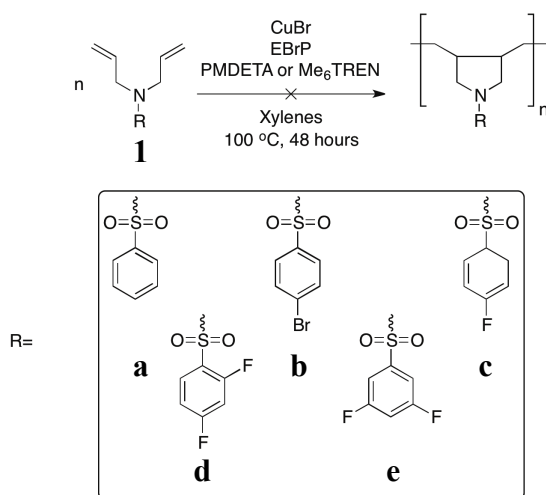
3.1.5. ATRP and ICAR ATRP Polymers

3.1.5.1 ATRP of DABSA Derivatives

The atom transfer radical polymerization (ATRP) of **1a-e** was conducted as outlined in **Scheme 18**. For each of the reactions, commercially available *N,N,N',N',N''*-pentamethyldiethylenetriamine (PMDETA) or tris[2-(dimethylamino)ethyl]amine (Me_6TREN) in xylenes was added to a Schlenk tube containing CuBr , ethyl-2-

bromopropionate (EBrP), and the appropriate DABSA derivative, and allowed to react at 100 °C for 48 hours. After 48 hours, the polymer was analyzed via ^1H NMR analysis, which showed no conversion of monomer to polymer.

ATRP owes its success to the transition metal catalyst, in this case CuBr, and nitrogen based ligand complex. Because the monomers used are also nitrogen based, they may be acting as an alternative ligand for the copper center, resulting in the ATRP being unsuccessful.

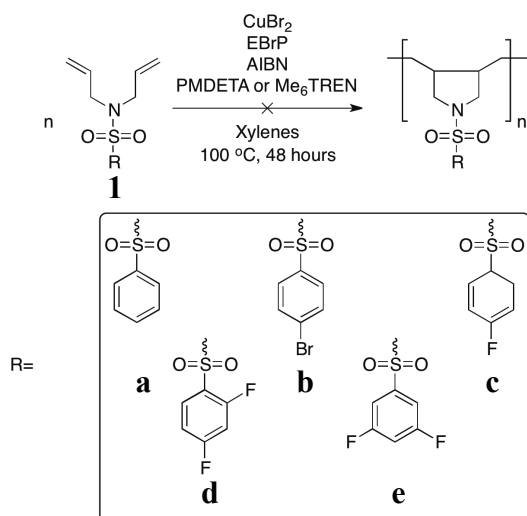


Scheme 18. ATRP of **1a-e**.

3.1.5.2 ICAR ATRP of DABSA Derivatives

The ICAR ATRP of **1a-e** was conducted as outlined in **Scheme 19**. For each of the reactions, commercially available PMDETA or Me₆TREN in xylenes was added to a Schlenk tube containing CuBr, EBrP, AIBN, and the appropriate DABSA derivative, and allowed to react at 100 °C for 48 hours. After 48 hours, the polymer was analyzed via ^1H NMR analysis, which showed no conversion of monomer to polymer.

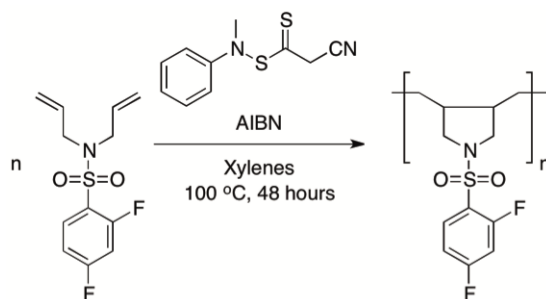
For reasons that were previously mentioned, ICAR ATRP was unsuccessful in polymerizing the monomers that were used.



Scheme 19. ICAR ATRP of **1a-e**.

3.1.6. RAFT of DABSA-2,4-DF

The reversible addition-fragmentation chain transfer (RAFT) polymerization of DABSA-2,4-DF (**1d**) was conducted as outlined in **Scheme 20**. For each of the reactions, commercially available cyanomethyl methyl(phenyl) carbamodithioate (CMMPCDT) in xylenes was added to a Schlenk tube containing AIBN and **1d** and allowed to react at 100 °C for 48 hours. After 48 hours, the polymer was analyzed via ^1H NMR analysis, which showed little conversion of monomer to polymer. The reaction was allowed to continue for 7 days, at which point the polymer was precipitated from diethyl ether to afford 0.016 g (2%) of **p2d**. The polymer was once again analyzed via ^1H NMR spectroscopy and GPC.



Scheme 20. RAFT polymerization of **1d**.

The ^1H NMR spectrum of RAFT polymerization of **1d** is shown in **Figure 14**. The spectrum indicates successful polymerization of **1d**, with a cyclization efficiency of 94.5%. The decrease in intensity of protons **a-c** indicates the polymerization of **1d**, while the residual allyl peaks indicate that 100% cyclization did not occur. Protons **d** and **e/f** appear as broad singlets from 7.84-8.00 ppm and 6.94-7.08, respectively. Protons **a'**, **b'**, and **c'** appear as a broad series of multiplets from 0.50-3.70 ppm. The broadening in the aromatic and aliphatic region are both stereotypical in cyclopolymerization. The additional peaks present in the aromatic region are attributed to the phenyl ring in CMMPCDT.

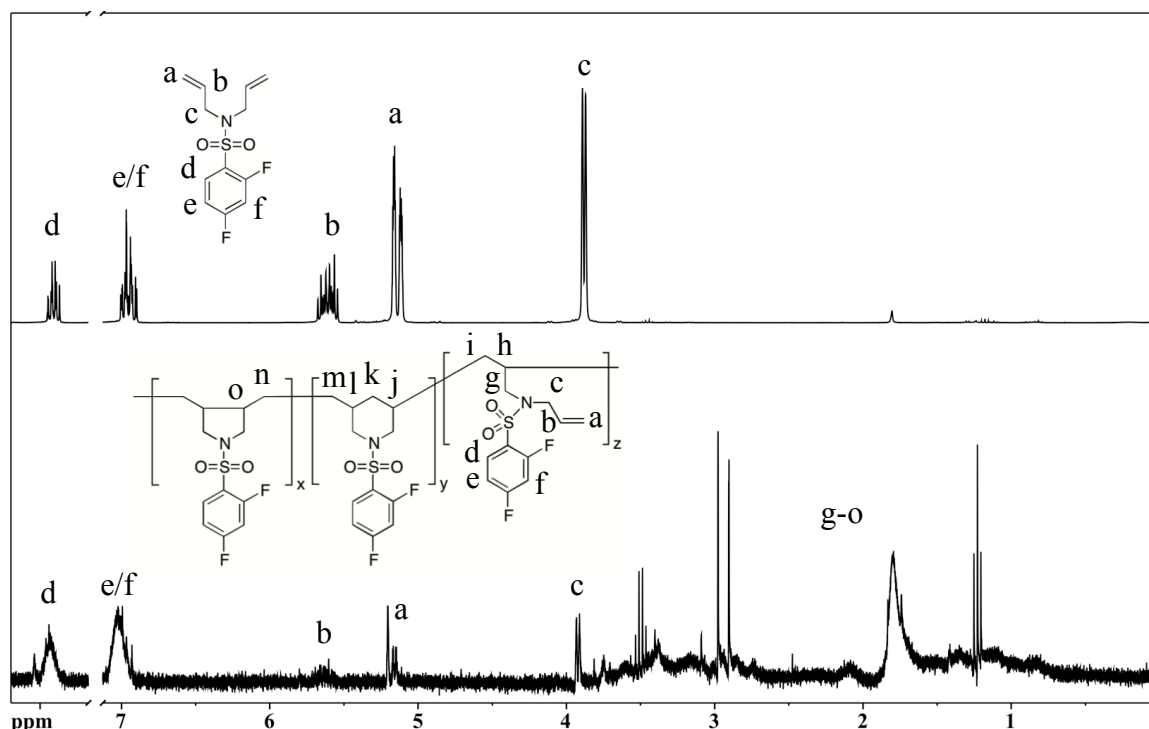
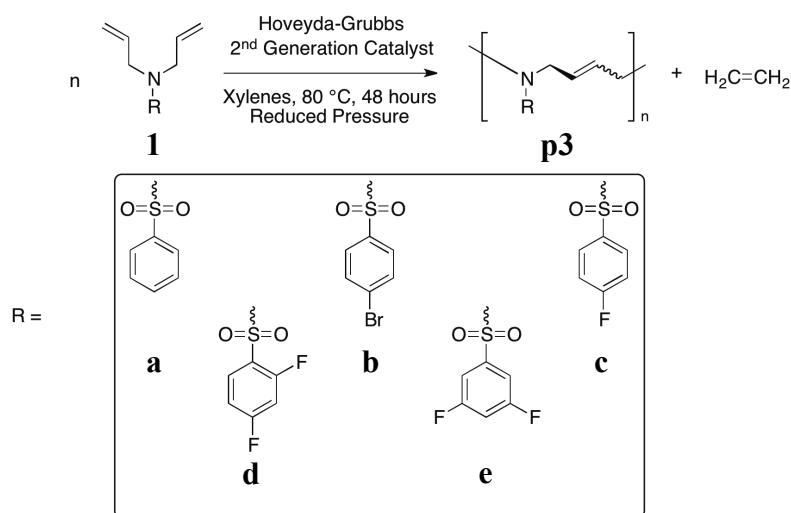


Figure 14. 300 MHz ^1H NMR spectra of **1d** (top) and **p2d** (bottom).

3.2. ADMET Polymers

Polymers **p3a-e** were prepared via the acyclic diene metathesis (ADMET) polymerization of monomers **1a-e**, as outlined in **Scheme 21**. For each of the reactions, commercially available Hoveyda-Grubbs 2nd generation catalyst was allowed to react

with the appropriate DABSA derivative at 70 °C for approximately 48 hours. The reaction was carried out under reduced pressure in order to remove the ethylene that builds up in the reaction, which can result in the formation of lower molecular weight polymers (**Scheme 6**). The polymers were precipitated from diethyl ether, centrifuged, washed again with diethyl ether, and isolated by the removal of diethyl ether via decantation and vacuum to afford an off-white solid. The structures were confirmed by ^1H and ^{13}C NMR spectroscopy, and integration of the ^1H NMR spectrum confirmed the correct number of hydrogens in the polymer.



Scheme 21. ADMET polymerization of monomers **1a-e**.

Polymer **p3a** was prepared in a 52% yield. The ^1H NMR spectrum contains six unique peaks (see **Figure 15**). Both protons **b'** (5.67 ppm) and **c'** (4.15 ppm) appear as singlets. Peaks **a** and **b** in the monomer ^1H NMR spectrum are consolidated into a single peak in the polymer ^1H NMR spectrum (**b'**), indicating the loss of ethylene, and the successful formation of polymer. The lack of splitting in **b'** and **c'** indicates that the allyl groups have been converted to alkenes, and could be indicative of a conformationally locked polymer structure (*i.e.* carbon-carbon double bond in the backbone is either in *cis*- or *trans*- conformation). As in the monomer spectrum, proton **d'** appears as a multiplet

from 7.83-7.88, and protons **e'** and **f'** appear as a series of broad, overlapping multiplets from 7.52-7.64 ppm, indicating that the phenyl ring was unaffected by the polymerization.

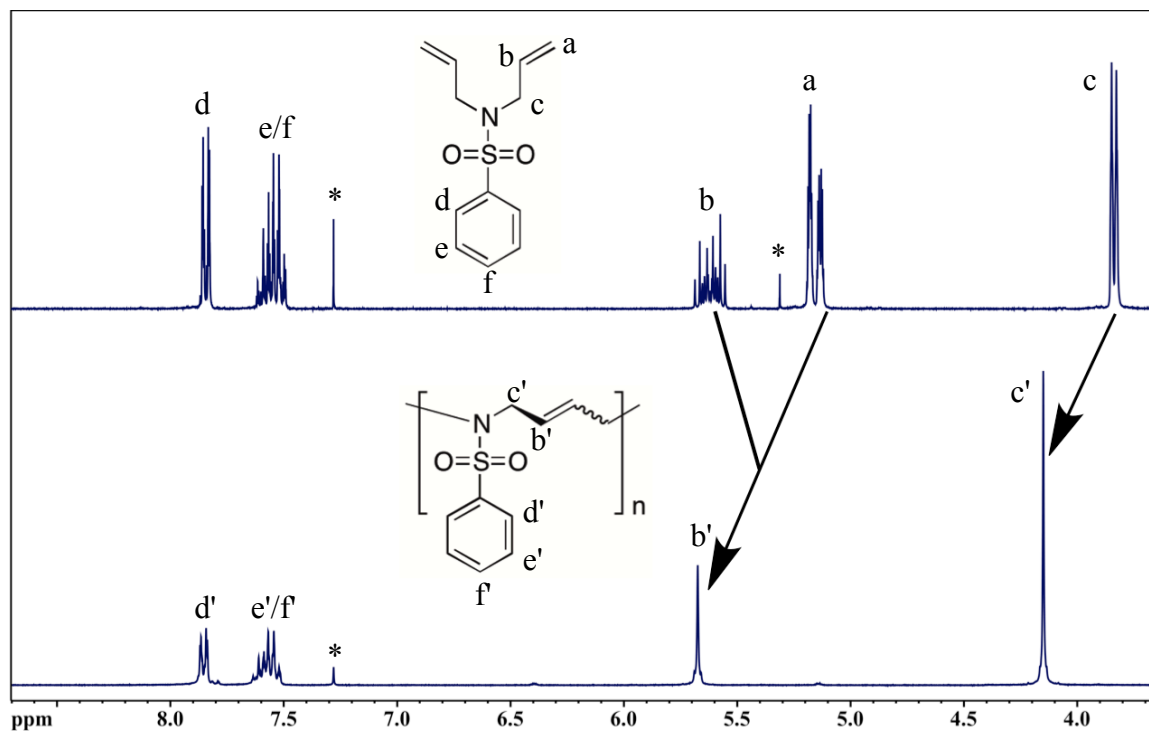


Figure 15. 300 MHz ^1H NMR spectral overlay (CDCl_3) of **1a** (top) and **p3a** (bottom).

ADMET polymerizations of the remaining *N,N*-diallylbenzenesulfonamide derivatives were carried out in an analogous fashion, and the major differences between the ^1H spectra (see **Figure 16**) are the specific signals in the aromatic region, arising from monomer used, with protons **b'** and **c'** appearing in essentially the same positions in each of the polymers.

Polymer **p3b** was prepared in a 54% yield; protons **d'** and **e'** appear as a series of broad, overlapping multiplets from 7.67-7.74 ppm. Polymer **p3c** was prepared in a 50% yield; proton **d'** and **e'** appear as a series of broad multiplets from 7.84-7.90 ppm and 7.18-7.25 ppm, respectively. Polymer **p3d** was prepared in a 40% yield; proton **d'** appears as a series of broad multiplets from 7.91-8.00 ppm, and protons **e'/f'** appear as a

series of broad, overlapping multiplets from 6.93-7.05 ppm. Polymer **p3e** was prepared in a 58% yield; proton **d'** appears as a series of broad multiplets from 7.35-7.43 ppm, and proton **e'** appears as a triplet of triplets at 7.06 ppm due to coupling with two equivalent *ortho*-fluorine atoms ($^2J_{\text{H-F}} = 2.34$ Hz) and two equivalent *meta*-hydrogen atoms ($^3J_{\text{H-H}} = 8.50$ Hz).

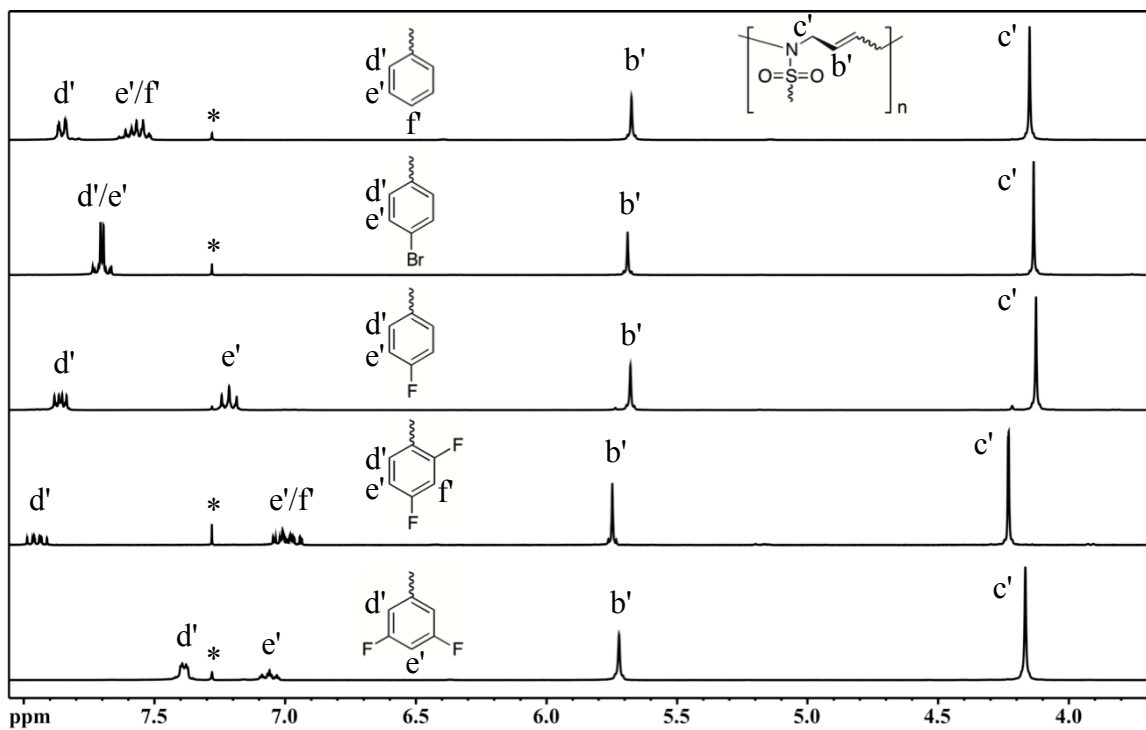


Figure 16. 300 MHz ^1H NMR spectral overlay (CDCl_3) of ADMET polymers **p3a-e**.

The ^{13}C NMR spectrum of **p3a** (**Figure 17**) contains six unique peaks. Peaks **a** and **b** in the monomer spectrum are consolidated into a single peak in the polymer spectrum (**b'**), indicating the loss of ethylene, and the successful formation of polymer. Carbons **b'** and **c'** appear as singlets at 125.4 and 54.9 ppm, respectively. Carbons **d'** at 137.3 ppm, **e'** at 127.3 ppm, **f'** at 129.1, and **g'** at 132.7 also appear as singlets, as they do in the ^{13}C NMR spectrum of **1a**, indicating that the phenyl ring was unaffected by the polymerization.

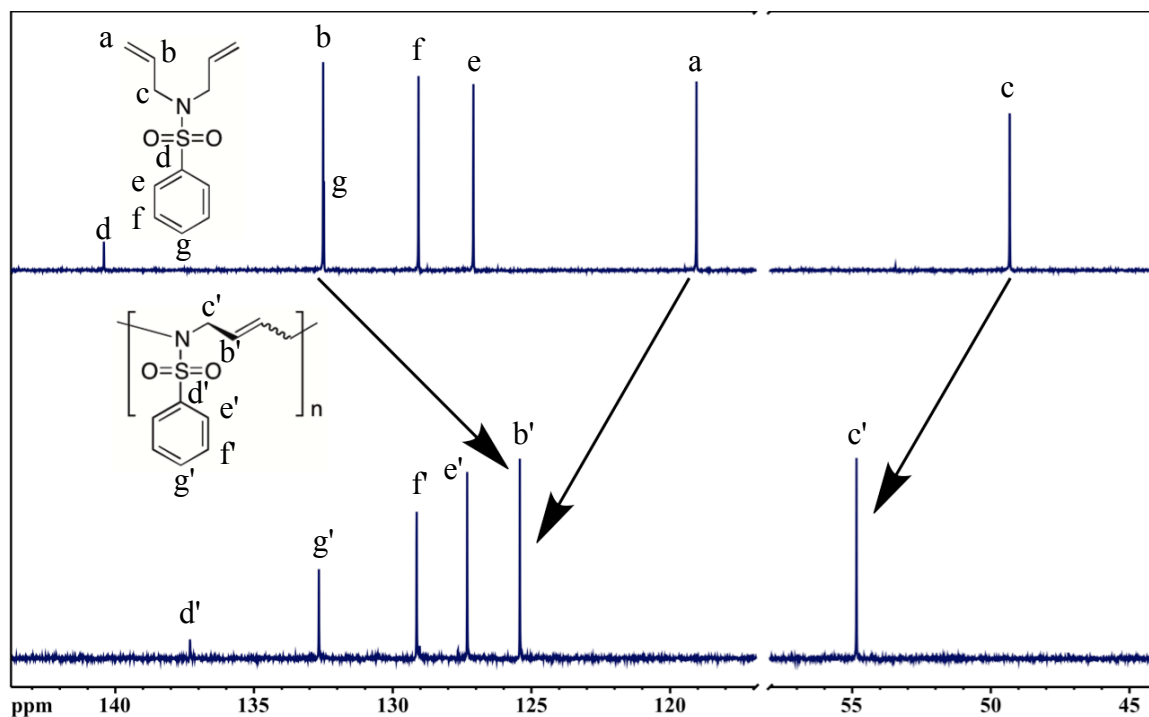


Figure 17. 75.5 MHz ¹³C NMR spectra (CDCl₃) of **1a** (top) and **p3a** (bottom).

The major differences between the ¹³C spectra (see **Figure 18**) are the specific signals in the aromatic region, arising from monomer used, with carbons **b'** and **c'** appearing in essentially the same positions in each of the polymers.

In the ¹³C NMR spectrum of **p3b**, carbons **d'**, **e'**, and **f'** appear as singlets at 136.4, 128.8, and 132.4 ppm, respectively. In the ¹³C NMR spectrum of **p3c**, carbon **d'** appears as a singlet at 133.5 ppm, carbon **e'** appears as a doublet at 130.0 ppm (³J_{C-F} = 9.28 Hz) due to coupling with a *meta*-fluorine atom, carbon **f'** appears as a doublet at 116.4 ppm (²J_{C-F} = 22.5 Hz) due to coupling with an *ortho*-fluorine atom, and carbon **g'** appears as a doublet at 165.1 ppm (¹J_{C-F} = 255 Hz) due to coupling with an *ipso*-fluorine atom. In the ¹³C NMR spectrum of **p3d**, carbon **d'** appears as a multiplet from 122.8-123.1 ppm, and carbons **e'** at 132.9 ppm (³J_{C-F} = 2.24, ³J_{C-F} = 10.3 Hz), **f'** at 111.7 ppm (²J_{C-F} = 3.81 Hz, ⁴J_{C-F} = 21.8 Hz), **g'** at 165.6 ppm (¹J_{C-F} = 11.4 Hz, ³J_{C-F} = 166 Hz) and carbon **i'** at 159.7 ppm (¹J_{C-F} = 12.7 Hz, ³J_{C-F} = 258 Hz) appear as doublets of doublets

due to coupling with two non-equivalent fluorine atoms and carbon **h** appears as a triplet at 105.7 ppm ($^2J_{C-F} = 25.7$ Hz) due to coupling with two equivalent fluorine atoms. In the ^{13}C NMR spectrum of **p3e**, carbons **d'** at 140.7 ppm ($^3J_{C-F} = 7.79$ Hz) and **g'** at 108.3 ppm ($^2J_{C-F} = 25.1$ Hz) appear as triplets due to coupling with two equivalent fluorine atoms, and carbons **e'** at 110.7 ppm ($^2J_{C-F} = 9.36$ Hz, $^4J_{C-F} = 18.2$ Hz) and **f'** at 162.9 ppm ($^1J_{C-F} = 11.64$ Hz, $^3J_{C-F} = 255$ Hz) appear as doublets of doublets due to coupling with two non-equivalent fluorine atoms.

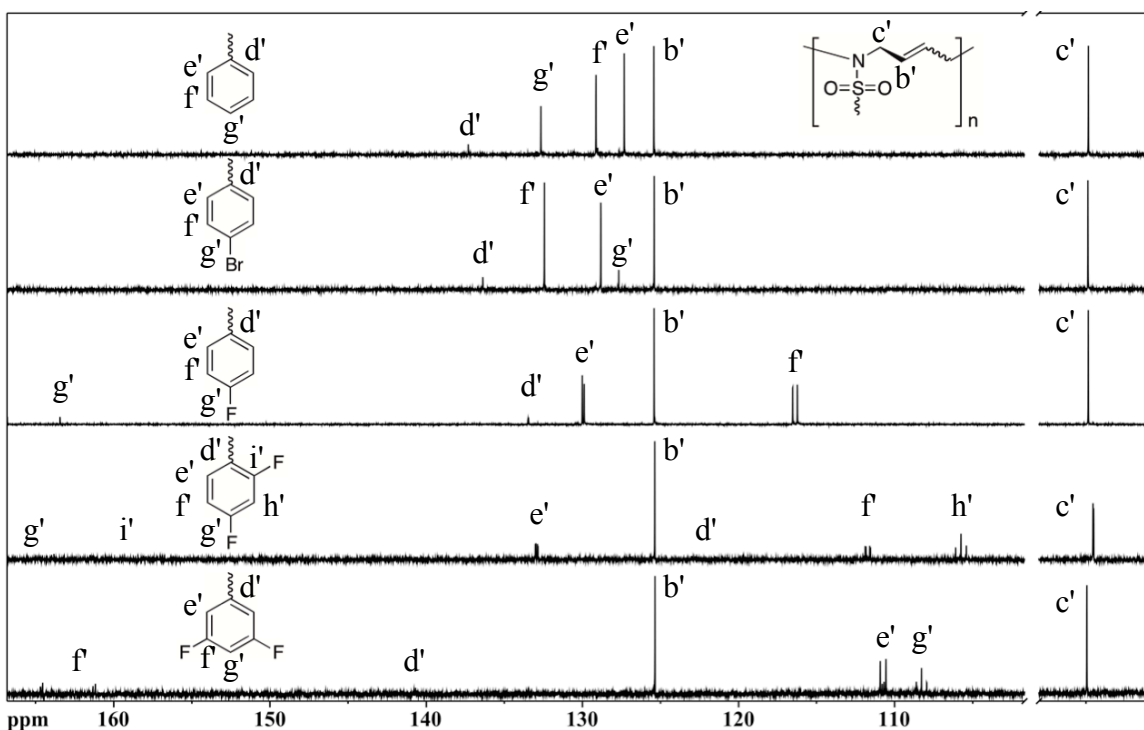
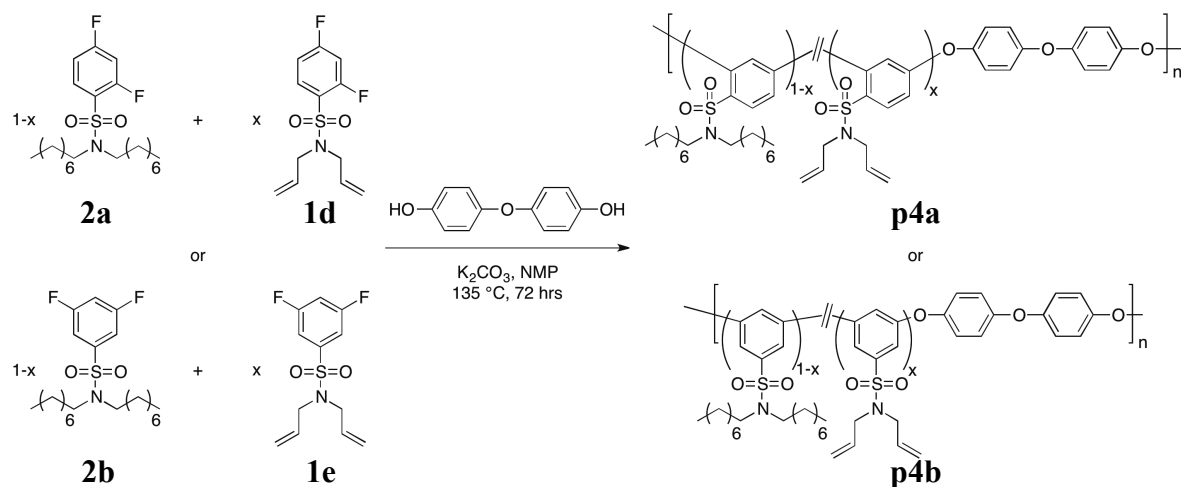


Figure 18. 75.5 MHz ^{13}C NMR spectral overlay ($CDCl_3$) of ADMET polymers **p3a-e**.

3.3. S_NAr Copolymers

Copolymers **p4a** and **p4b** were prepared via the S_NAr copolymerization of **1d/2a** or **1e/2b** in a 95/5 ratio using 4,4'-dihydroxydiphenyl ether, as shown in **Scheme 22**. The reagents were heated to 135 °C in order to prevent crosslinking of the allyl groups. After 72 hours, DEPT 90 ^{13}C NMR spectroscopy showed no residual starting material, as indicated by the absence of the triplet present in the starting material. The structure of the

polymers were confirmed by ^1H and DEPT 90 ^{13}C NMR spectroscopy, and the polymers were characterized by GPC, TGA, and DSC analyses.



Scheme 22. $\text{S}_{\text{N}}\text{Ar}$ copolymerization of **2a/b** and **1d/e** to form **p4a/b**.

3.3.1. $\text{S}_{\text{N}}\text{Ar}$ Copolymerization of **1d** and **2a** using 4,4'-dihydroxydiphenyl ether

The ^1H NMR spectrum of **p4a** (**Figure 19**) contains eleven distinct peaks. Protons **a** and **b** from 6.94-7.11, **c** from 0.84-0.91 ppm, **i** from 1.47-1.60 ppm, **j** from 3.25-3.30 ppm, **l** from 5.63-5.75 ppm, and **p** from 6.49-6.58 ppm appear as a series of broad multiplets. Protons **d**, **e**, **f**, **g**, and **h** appear as a singlet at 1.24 ppm, as does proton **o** at 7.28 ppm. Protons **k** at 5.17 ppm ($^3J_{\text{H-H}} = 13.20$ Hz), **m** at 3.96 ppm ($^3J_{\text{H-H}} = 6.01$ Hz), and **n** at 7.92 ppm ($^3J_{\text{H-H}} = 8.40$ Hz) appear as doublets due to coupling with an adjacent proton. Due to coupling with both the *ipso*-proton, as well as an adjacent proton, proton **k** has a larger coupling constant than either **m** or **n**.

Protons **c-l** appear in essentially the same positions in **p4b**, with the major differences being in the aromatic region. Protons **a** and **b** from 6.94-7.23, **n** from 6.72-6.86 ppm, and **o** from 6.94-7.23 ppm appear as multiplets.

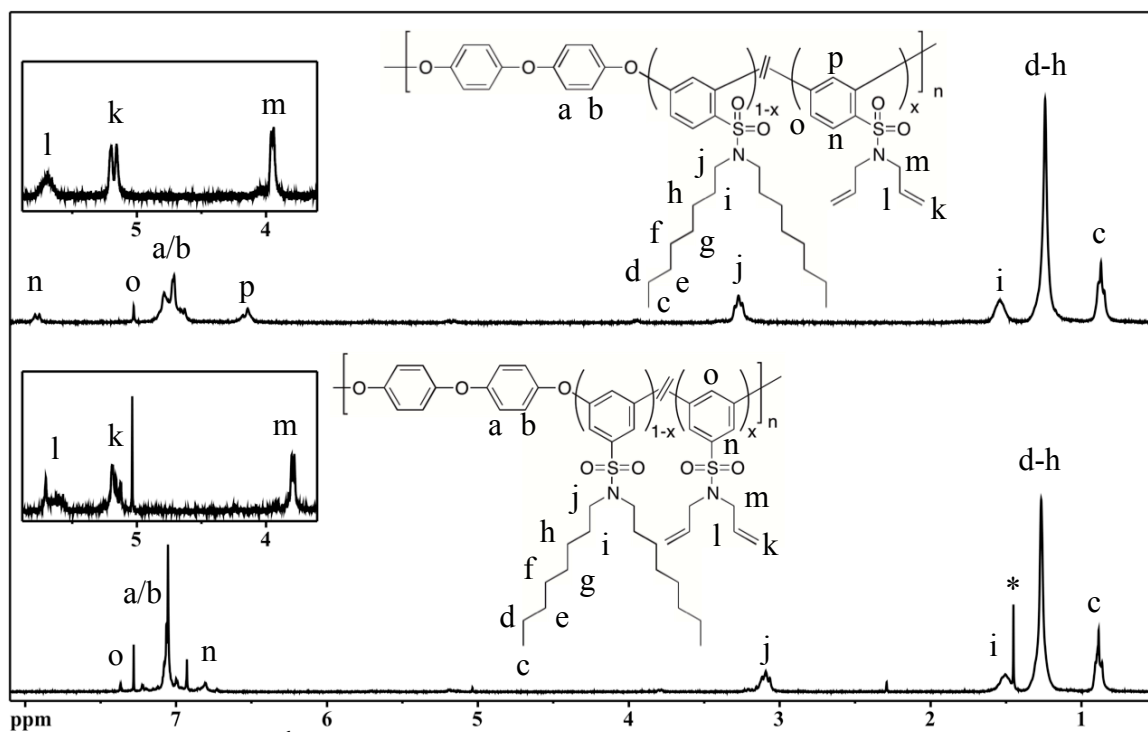


Figure 19. 300 MHz ^1H NMR (CDCl_3) spectral overlay of **p4a** (top) and **p4b** (bottom).

In the DEPT 90 ^{13}C NMR spectrum of **p4a** (Figure 20), carbons **a**, **b**, **c**, and **d** appear as singlets at 132.9, 120.2, 109.5 and 107.0 ppm, respectively. Carbons **e** and **f** appears as a doublet at 121.6 ppm ($^2J_{\text{C-O}} = 8.15$ Hz) because of the difference in chemical shift associated with coupling with an *ortho*- and *para*- sulfonamide. In the DEPT 90 ^{13}C spectrum of **p4b** (Figure 21), carbons **a**, **b**, **c**, and **d/e** appear as singlets at 136.0, 110.0, 110.7, and 121.4 ppm, respectively.

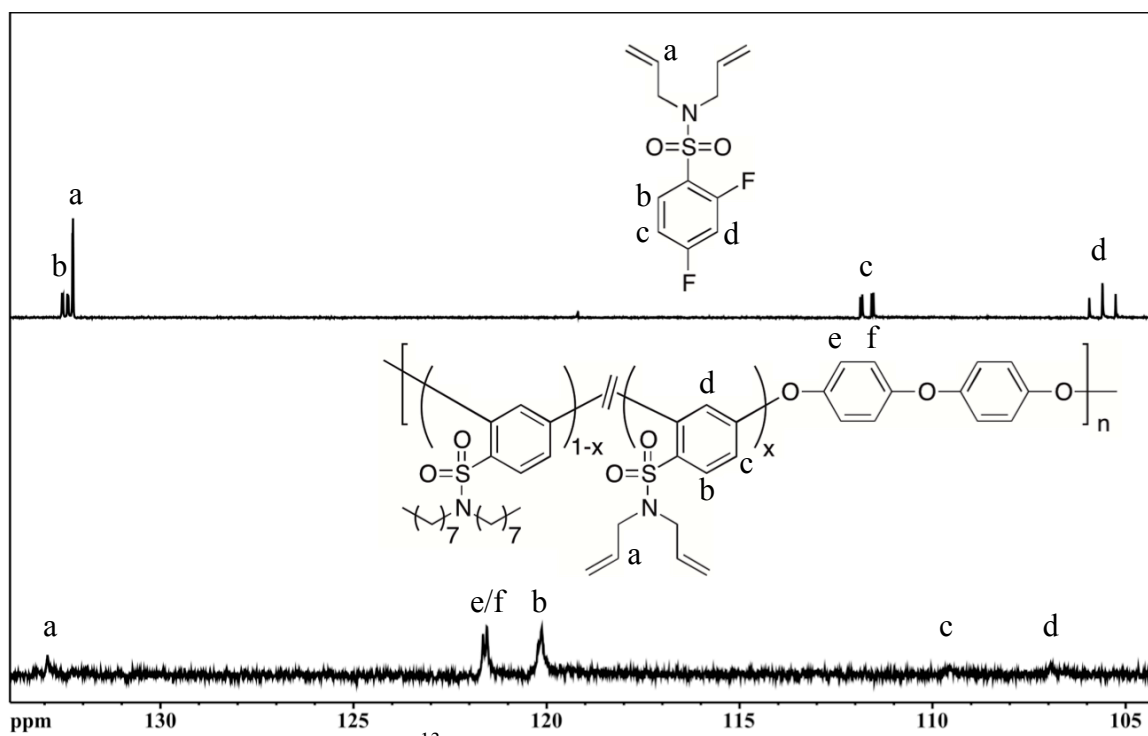


Figure 20. 75.5 MHz DEPT 90 ^{13}C NMR (CDCl_3) spectral overlay of **1d** (top) and **p4a** (bottom).

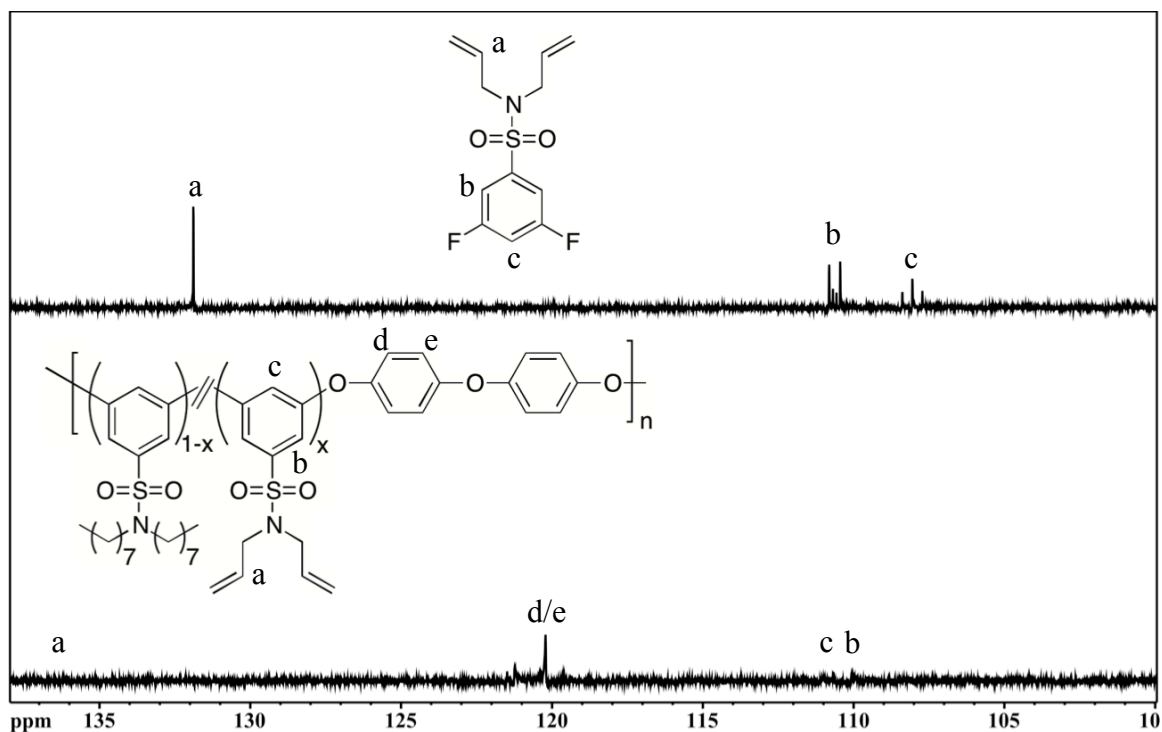


Figure 21. 75.5 MHz DEPT 90 ^{13}C NMR (CDCl_3) spectral overlay of **1e** (top) and **p4b** (bottom).

3.4. Polymer Molecular Weights and Thermal Properties

The polymers were further analyzed using gel permeation chromatography (GPC), differential scanning calorimetry (DSC), and thermogravimetric analysis (TGA). Characterization data, including number and weight average molecular weight (M_n and M_w , respectively), dispersity (D), cyclization efficiency (CE), glass transition temperature (T_g), melting temperature (T_m), and the 5% weight loss ($T_{d-5\%}$) are summarized in **Tables 3-7**.

GPC was used to determine molecular weight and molecular weight distributions of polymers soluble in THF/5% acetic acid. The D and M_w were determined using the refractive index (RI) and light-scattering detectors. For the free radical polymers, the M_w was found to be from 1,421 to 5,079 g/mol, with D values ranging from 1.78-3.31. In both the AIBN and BPO initiated polymers, *N,N*-diallyl-3,5-difluorobenzenesulfonamide (**1e**) afforded the highest M_w polymers, whereas *N,N*-diallylbenzenesulfonamide (**1a**) afforded the lowest. By comparing the calculated electrostatic charge and differences in chemical shift between the terminal and penultimate allyl carbons, the difference in molecular weight can be explained. Although the calculated charge on the nitrogen is more negative for **1e** than it is on **1a-d**, the actual chemical shifts explain the difference in molecular weight. As previously stated, Mathias *et al.* showed that the smaller the difference in chemical shift in the allyl groups, the lower the propensity for chain transfer via hydrogen abstraction from the allyl position, resulting in an increase in molecular weight of the resulting polymer.

Table 3. Differences in chemical shift and molecular weights of free radical polymers.

	$\Delta\delta$ (ppm)	Electrostatic Charge	Initiator	M_n (g/mol)	M_w (g/mol)	D	Yield (%)	CE (%)
p1a	13.5	-0.105	AIBN	700	1,431	2.04	33	97.5
			BPO	1,128	2,003	1.78	24	98.9
p1b	13.1	-0.138	AIBN	820	2,010	2.45	24	97.8
			BPO	-	-	-	-	-
p1c	13.1	-0.131	AIBN	994	2,158	2.17	35	97.9
			BPO	-	-	-	-	-
p1d	13.1	-0.134	AIBN	1,497	3,420	2.28	29	99.2
			BPO	1,209	2,976	2.46	21	99.1
p1e	12.3	-0.139	AIBN	1,325	4,386	3.31	37	98.8
			BPO	1,630	5,079	3.12	28	98.7

The thermal stability of the polymers, reported as 5% decomposition temperature ($T_{d-5\%}$) under nitrogen was investigated using thermogravimetric analysis (TGA), while the glass transition temperatures (T_g) were determined using differential scanning calorimetry (DSC).

Overlays of the thermal analyses of AIBN and BPO initiated polymers are shown in Figures 22-25.

The glass transition temperatures (T_g) ranged from 86 °C for BPO initiated DABSA (see **Figure 22**) to 114 °C for AIBN initiated DABSA-4-Br (see **Figure 24**). The higher T_g can be attributed to a more rigid polymer backbone.

The free radical polymers showed moderate thermal stability above 290 °C for AIBN initiated polymers (see **Figure 23**), and 262 °C for BPO initiated polymers (see **Figure 25**) under nitrogen atmosphere. For AIBN initiated polymers, the $T_{d-5\%}$ for the first degradation step ranged from 290 °C for **p1c** to 305 °C for **p1d**, while the BPO initiated polymers ranged from 262 °C for **p1a** to 302 °C for **p1d**.

Table 4. Thermal data for free radical polymers.

	Initiator	T _g (°C)	T _{d-5%} (°C)
p1a	AIBN	94	292
	BPO	86	262
p1b	AIBN	114	303
	BPO	-	-
p1c	AIBN	87	290
	BPO	-	-
p1d	AIBN	112	305
	BPO	111	302
p1e	AIBN	87	302
	BPO	98	287

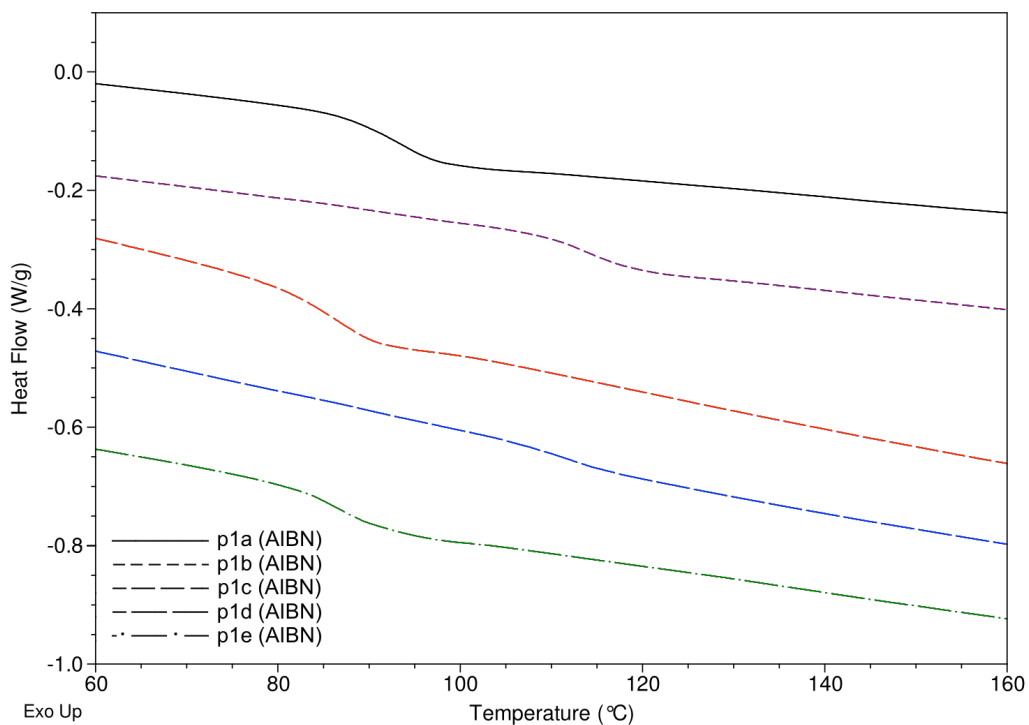


Figure 22. DSC results of AIBN initiated DABSA derivatives.

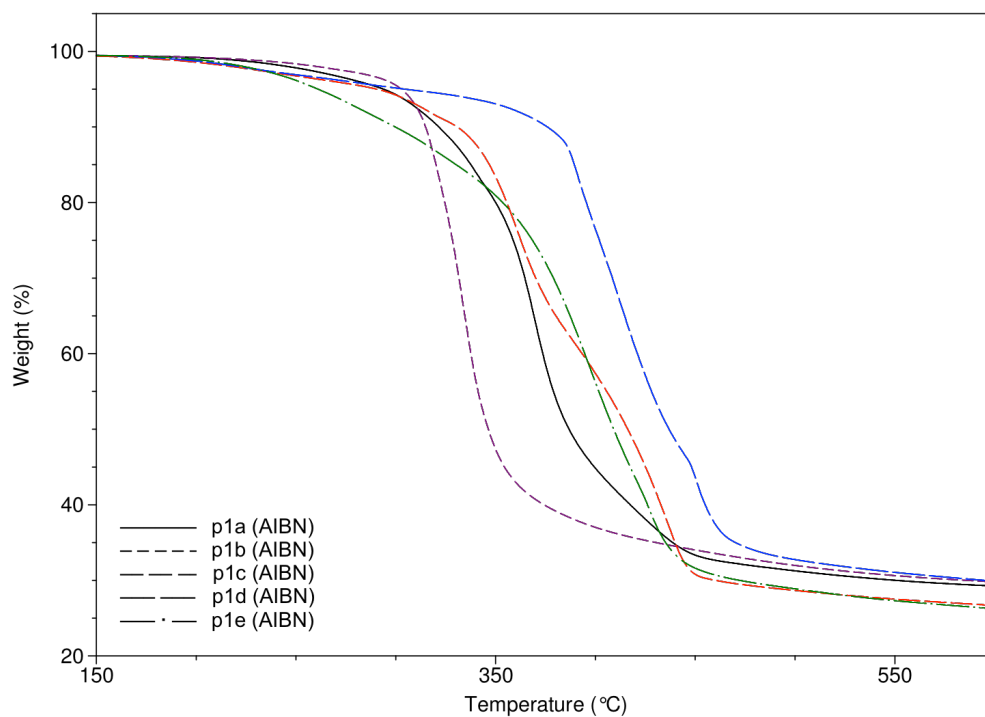


Figure 23. TGA results of AIBN initiated DABSA derivatives.

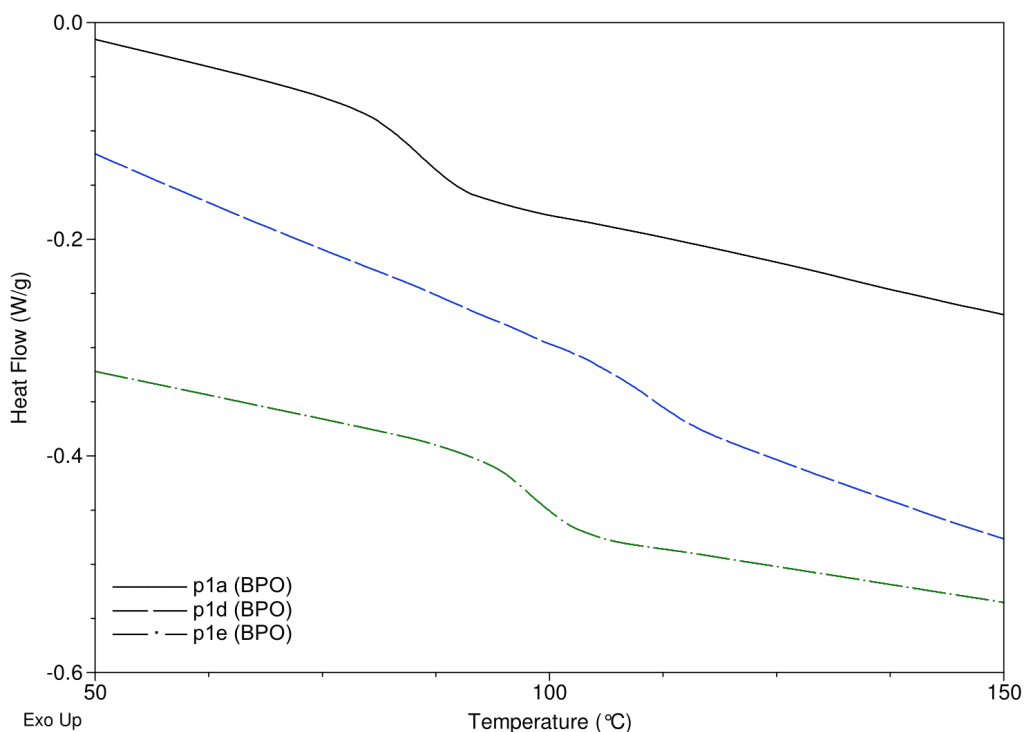


Figure 24. DSC results of BPO initiated DABSA derivatives.

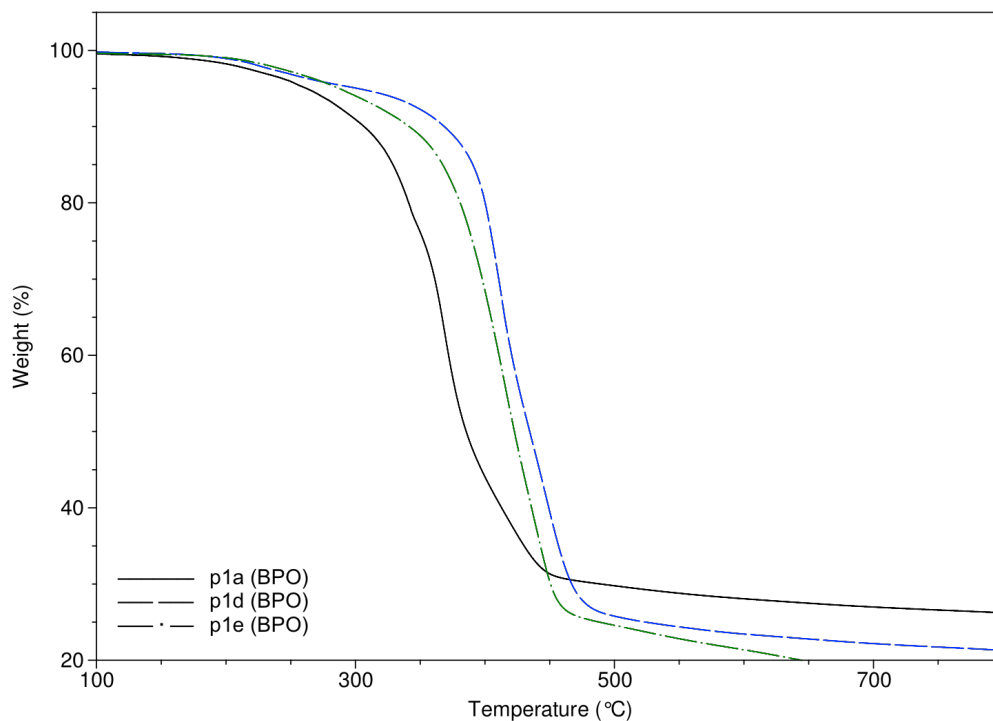


Figure 25. TGA results of BPO initiated DABSA derivatives.

For the RAFT polymer of DABSA-2,4-DF, the M_w was found to be 1,154 g/mol, with a dispersity of 1.47. The low molecular weight may be attributed to the selection of RAFT transfer agent (RTA), by selecting an alternative RTA such as 2-(dodecylthiocarbonothioylthio)-2-methylpropionic acid, which is well suited for the RAFT polymerization of acrylamides.

Table 5. Molecular weight of RAFT polymer **p2d**.

	M_n (g/mol)	M_w (g/mol)	\mathcal{D}
DABSA-2,4-DF	786	1,154	1.47

For the ADMET polymers, the M_w was found to be from 10,150 to 30,229 g/mol, with \mathcal{D} values ranging from 1.24-2.03. *N,N*-diallylbenzenesulfonamide (**1a**) afforded the highest M_w polymers, whereas *N,N*-diallyl-2,4-difluorobenzenesulfonamide (**1d**) afforded the lowest. Due to the *ortho*- and *para*- fluorine atoms in monomer **1d**, the structure is

asymmetric. This could limit the ability of the catalyst to convert monomer to polymer, resulting in the decrease in molecular weight.

Table 6. Molecular weights and thermal properties of ADMET polymers.

	M_n (g/mol)	M_w (g/mol)	D	T_m (°C)	$T_{d-5\%}$ (°C)
DABSA	14,915	30,229	2.03	115	146
DABSA-4-Br	8,692	14,168	1.63	136	167
DABSA-4-F	17,075	28,966	1.70	90	159
DABSA-2,4-DF	5,547	10,150	1.86	65.5	171
DABSA-3,5-DF	10,210	13,637	1.34	109	125

Melting temperatures (T_m) were determined using differential scanning calorimetry (DSC), and are shown in **(Figure 26)**.

The melting temperature (T_m) of the ADMET polymers ranged from 65.5 °C for **p3d** to 136 °C **p3b**. The lower T_m associated with **p3d** is, as previously stated, due to steric effects associated with monomer **1d**.

The ADMET polymers showed low thermal stability above 125 °C for under nitrogen atmosphere. The $T_{d-5\%}$ for the first degradation step ranged from 125 °C for **1e** to 171 °C for **1d**. As shown in **Figure 27**, the difference in degradation temperature between **1c** and **p3c** is minimal (152 and 157 °C, respectively), which can be explained through the structure of the polymer. The similarity of the polymer structure to that of the monomer (see **Scheme 21**) results in the degradation of the polymer being only slightly higher than the monomer. The TGA thermogram of ADMET polymers under nitrogen atmosphere is shown in **Figure 28**.

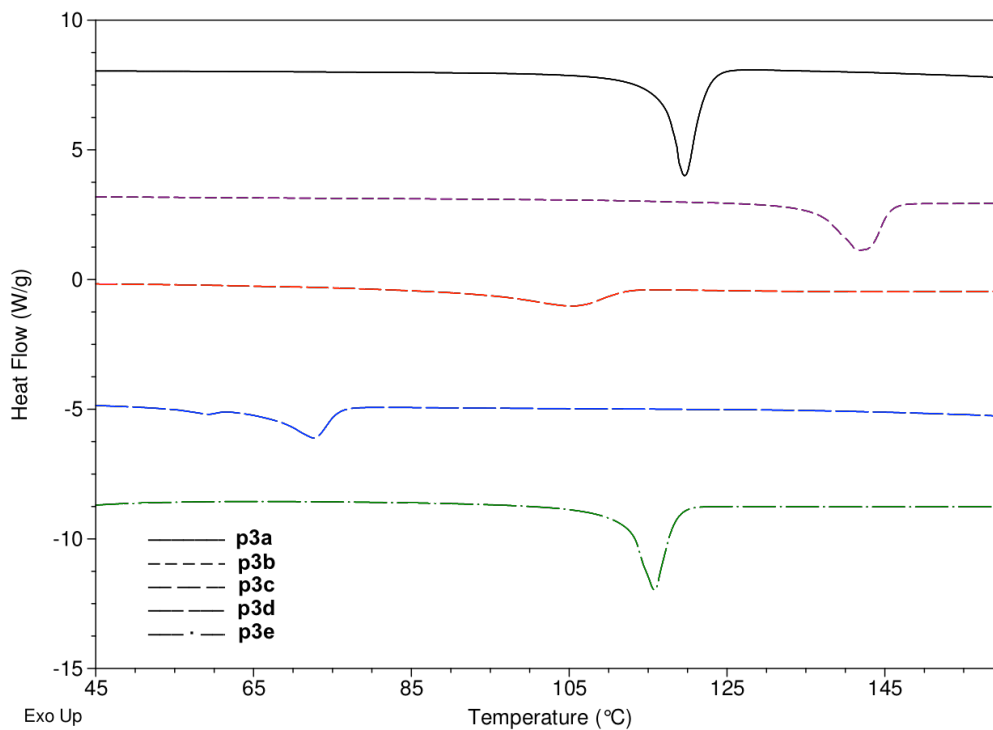


Figure 26. DSC results of ADMET polymers.

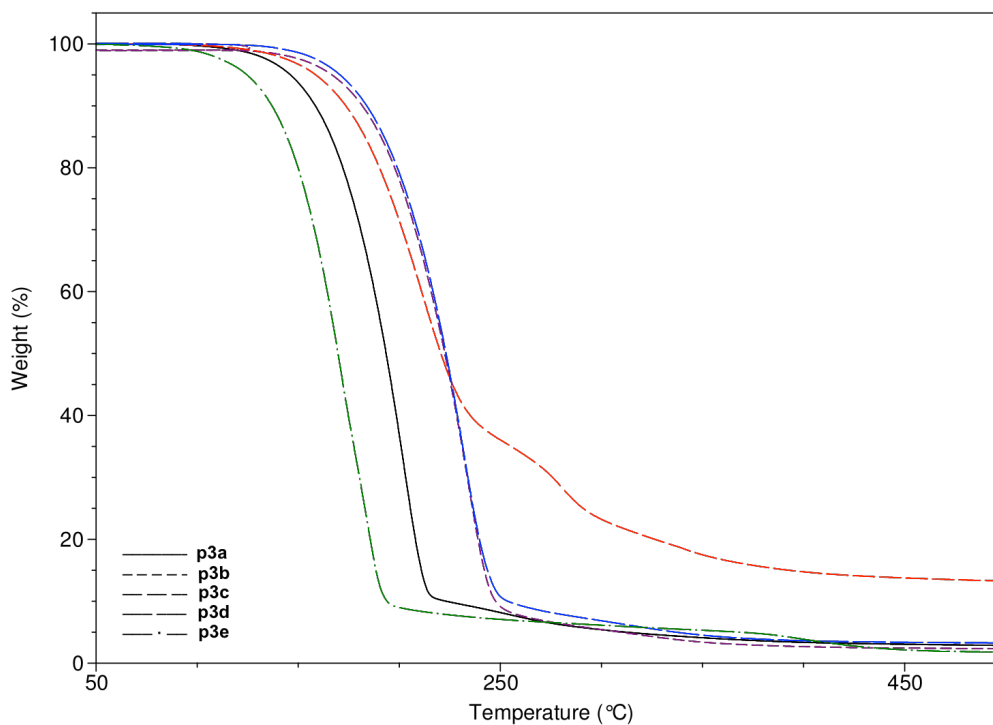


Figure 27. TGA results of **1c** and **p3c**.

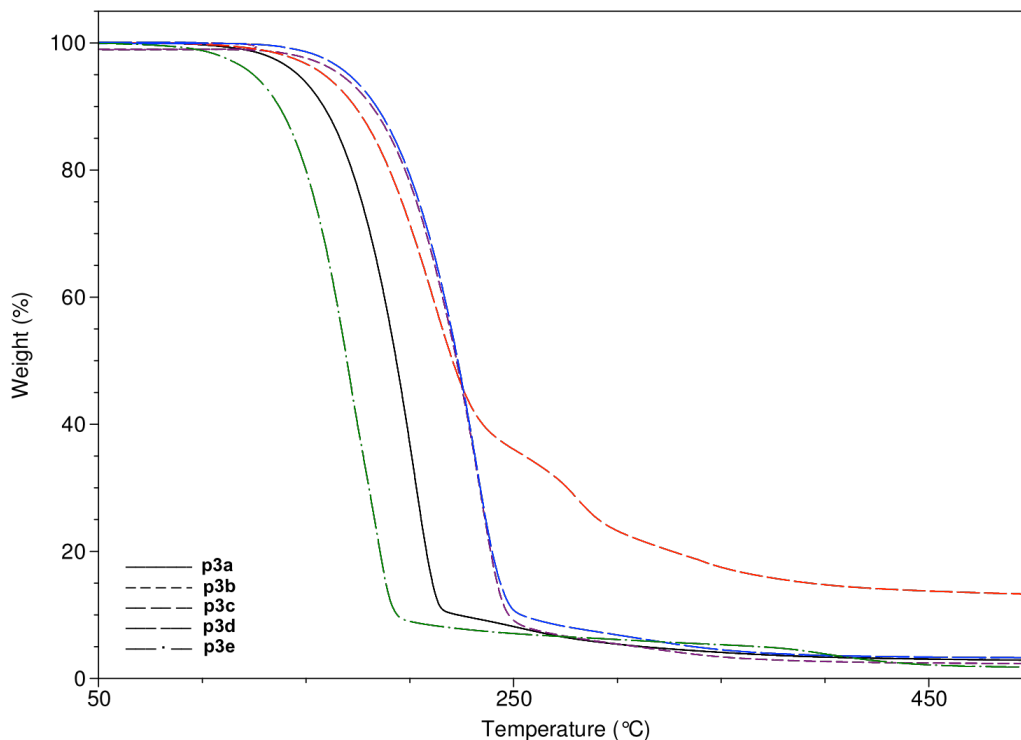


Figure 28. TGA results of ADMET Polymers.

As shown in **Table 7**, the M_w of the S_NAr copolymers were 7,440 g/mol for **p4b** and 9,530 g/mol for **p4a**, with D values ranging from 2.44-2.60.

Table 7. Molecular weights and thermal properties of S_NAr polymers.

Polymer	Monomer Components	Ratio	M_n (g/mol)	M_w (g/mol)	D	T_g (°C)	$T_{d-5\%}$ (°C)
p4a	2a:1d	95:5	3,660	9,530	2.60	14.5	354
p4b	2b:1e	95:5	3,050	7,440	2.44	6.34	329

Glass transition temperatures (T_g) were determined using differential scanning calorimetry (DSC) and overlays of S_NAr copolymers are shown in **Figure 29**.

The glass transition temperatures (T_g) were 70.3 °C for **p4b** and 96.3 °C for **p4a**. The higher T_g can be attributed to a more rigid polymer backbone, resulting from the incorporation of a greater amount of monomer into the polymer.

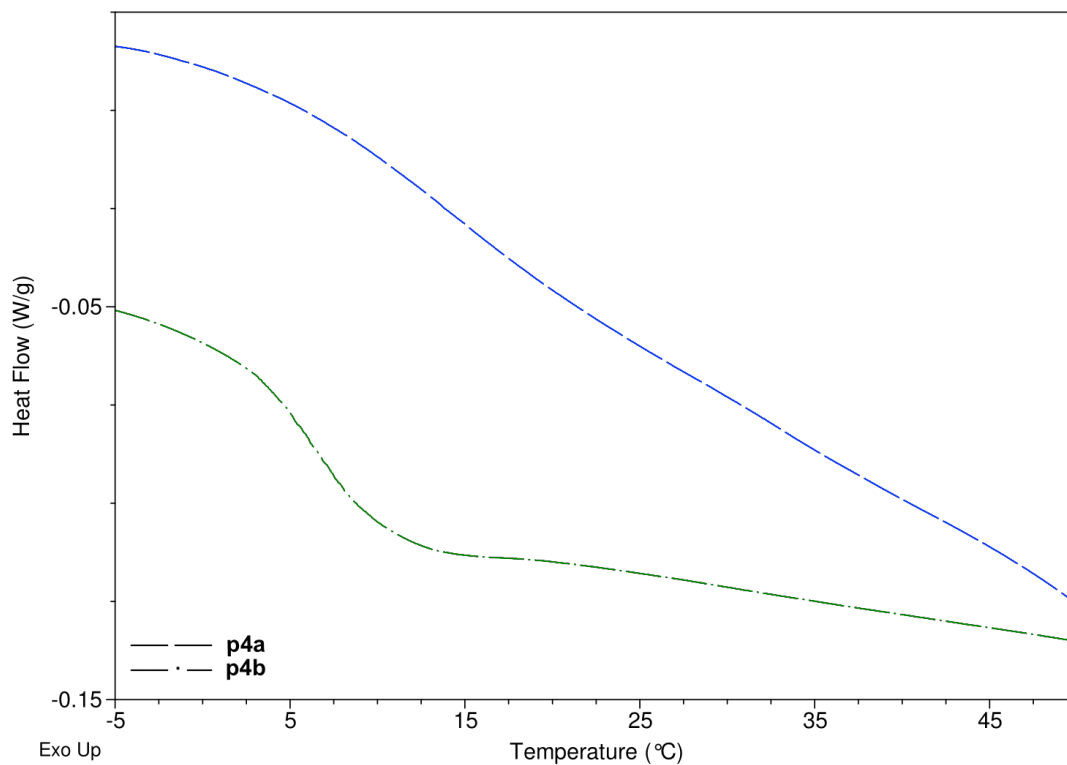


Figure 29. DSC results of S_NAr copolymers.

The S_NAr copolymers showed moderate thermal stability above 329 °C under nitrogen atmosphere. The $T_{d-5\%}$ for the first degradation step ranged from 329 °C for **p4b** to 354 °C for **p4a**. The TGA thermogram of S_NAr copolymers under nitrogen atmosphere is shown in **Figure 30**.

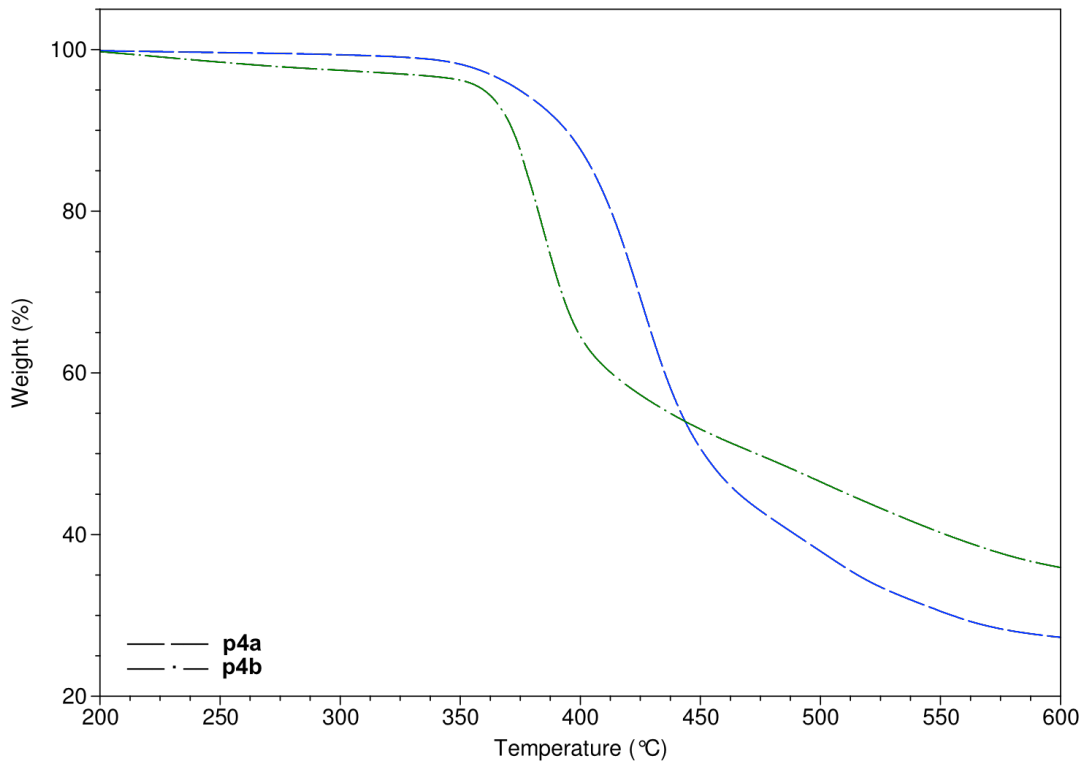


Figure 30. TGA results of S_NAr copolymers.

4. CONCLUSIONS

A series of sulfonamide based bifunctional monomers was successfully synthesized and polymerized via free radical (FRP), acyclic diene metathesis (ADMET), reversible addition-fragmentation chain transfer (RAFT), and nucleophilic aromatic substitution (S_NAr) polymerization processes. The weight average molecular weights, as determined by GPC, ranged from 1,430 Da to 5,070 Da, with D values ranging from 2.04-3.31 for FRP polymers; 13,640 Da to 30,230 Da, with D values ranging from 1.3 to 2.0 for ADMET polymers; 1,150 Da, with a D value of 1.47 for RAFT; and 7,440 to 9,530 Da, with D values ranging from 2.44 to 2.60 for S_NAr .

Thermal properties for the resulting polymers were determined by TGA and DSC with TGA analysis showing the polymers prepared via FRP possessed moderate thermal stability above 260 °C; polymers prepared via ADMET possessed relatively low thermal stability above 125 °C; and polymers prepared via S_NAr possessed better thermal stability above 330 °C.

DSC analysis showed that polymers prepared via FRP were amorphous, with glass transition temperatures ranging from a low of 87 °C for the AIBN initiated polymer of *N,N*-diallyl-3,5-difluorobenzenesulfonamide to a high of 114 °C for the polymer of *N,N*-diallyl-4-bromobenzenesulfonamide. The copolymers prepared via S_NAr were also found to be amorphous, with glass transition temperatures of 6 °C for the 3,5-difluoro copolymer to a high of 12 °C for the 2,4-difluoro copolymer. DSC analysis also showed

that polymers prepared via ADMET were crystalline, with melting temperatures ranging from a low of 65.5 °C for the polymer of *N,N*-diallyl-2,4-difluorobenzenesulfonamide to 136 °C for the polymer of *N,N*-diallyl-4-bromobenzenesulfonamide.

5. FUTURE WORK

S_NAr copolymers carrying pendent allyl groups can undergo further modification via post polymerization modification chemistry, such as thiol-ene click chemistry, and could incorporate various functional groups by changing the thiol chosen. These polymers may also be crosslinked after polymerization by the addition of a multifunctional thiol. Alternatively, polymers formed via radical or ADMET polymerization that carry pendent, functionalized benzene moieties can undergo various types of post polymerization modification such as S_NAr .

6. REFERENCES

1. Odian, G. *Principles of Polymerization*, 4th ed.; Wiley-Interscience: New Jersey, **2004**.
2. Fischer, H. *Macromolecules*, **1997**, *30*, 5666-5672.
3. Kato, M.; Kamigaito, M.; Sawamoto, M.; Higashimura, T. *Macromolecules*, **1995**, *28*, 1721.
4. Wang, J. S.; Matyjaszewski, K. *Macromolecules*, **1995**, *28*, 7901.
5. Percec, V.; Barboiu, B. *Macromolecules*. **1995**, *28*, 7970.
6. Moad, G.; Solomon, D. H. *The Chemistry of Radical Polymerization*, 2nd ed. Elsevier: Oxford, UK. **2006**.
7. Pintauer, T.; Matyjaszewski, K. *Chem. Soc. Rev.* **2008**, *37*, 1087-1097.
8. Carnegie Mellon University. Matyjaszewski Polymer Group: ARGET ATRP and ICAR ATRP. <https://www.cmu.edu/maty/atrp-how/procedures-for-initiation-of-ATRP/arget-icar.html> (accessed May 10, 2016).
9. Moad, G.; Ercole, F.; Johnson, C. H.; Krstina, J.; Moad, C. L.; Rizzardo, E.; Spurling, T. H.; Thang, S. H.; Anderson, A. G. *ACS Symp. Ser.* **1998**, *685*, 332.
10. Chiefari, J.; Chong, Y.K.; Ercole, F.; Krstina, J.; Jeffery, J.; Le, T. P. T.; Mayadunne, R. T. A.; Meijs, G. F.; Moad, C. L.; Moad, G.; Rizzardo, E.; Thang, S. H. *Macromolecules*, **1998**, *31*, 5559.

11. Butler, G. R.; Angelo, R. J. *J. Am. Chem. Soc.* **1956**, *79*, 3128.
12. Hawthorne, D. G.; Johnson, S. R.; Solomon, D. H.; Willing, R. I. *Aust. J. Chem.* **1976**, *29*, 1955.
13. Vaidya, R. A.; Mathias, L. J. *J. Polym. Sci. Polym. Symp.* **1986**, *74*, 243.
14. Matsumoto, A. *Prog. Polym. Sci.* **2001**, *26*, 189.
15. Zubov, V. P.; Kumar, M. V.; Masterova, M. N.; Kabanov, V. A. *J. Macrom. Sci-Chem.* **1979**, 111-131.
16. Hodgkin, J. H.; Johns, S. R.; Willing, R. I. *Polym Bulletin.* **1982**, *7*, 353-359.
17. Avci, Duygu; Haynes, C.; Mathias, L. J. *J. Polym Sci. A. Polym. Chem.* **1997**, *35* (10), 2111-2121.
18. Bouhadir, K. H.; Abramian, L.; Ezzedine, A.; Usher, K.; Vladimirov, N. *Macromol.* **2012**, *17*, 13290.
19. Crawshaw, A.; Jones, A. G. *J. Macromol. Sci. – Chem.* **1972**, *1*, 65.
20. Assem, Y.; Greiner, A.; Agarwal, S. *Macromol. Rapid Commun.* **2007**, *28*, 1923.
21. Matsoyan, S. G.; Pogosyan, G. M.; Dzhagalyan, A. O.; Mushegyan, A. V. *Polymer Science U.S.S.R.* **1963**, *4*, 1322.
22. Manas, C.; Salil, K. R. *Industrial Polymers, Specialty Polymers, and Their Applications; Plastics Engineering*, Vol. 73.; CRC Press:Boca Raton, FL. **2008**.
23. Mark, H. F. *Polysulfones; Encyclopedia of Polymer Science and Technology*, 4th Ed.; John Wiley & Sons, Inc.: New Jersey, **2003**; Vol. 4.

- ²⁴. Kaiti, S.; Himmelberg, P.; Williams, J.; Abdellatif, M.; Fossum, E. *Macromolecules*. **2007**, *39*, 7909.
- ²⁵. Beek, D. V.; Fossum, E. *Macromolecules*. **2009**, *42*, 4016.
- ²⁶. Tienda, K.; Yu, Z.; Constandinidis, F.; Fortney, A.; Feld, W. A.; Fossum, E. *J. Polym. Sci. Part A: Polym. Chem.* **2011**, *49*, 2908.
- ²⁷. Andrejevic, M.; Schmitz, J.; Fossum, E. *Mater. Today Commun.* **2015**, *3*, 10.
- ²⁸. Rebeck, N. T.; Knauss, D. M. *Macromolecules*. **2011**, *44*, 6717.
- ²⁹. Selhorst, R.; Fossum, E. *Polymer*. **2013**, *54*, 530.
- ³⁰. Hagiwara, T.; Suzuki, I.; Takeuchi, K.; Hamana, H.; Narita, T. *Macromolecules*. **1991**, *24*, 6856.
- ³¹. Jing, F.; Hillmyer, M. *J. Am. Chem. Soc.* **2008**, *130*, 13826.
- ³². Alkan, A.; Thomi, L.; Gleede, T.; Wurm, F. *Polym. Chem.* **2015**, *6*, 3617.
- ³³. Klein, R.; Ubel, F.; Frey, H. *Macromol. Rapid Comm.* **2015**, *36*, 1822.
- ³⁴. Sumerlin, B.; Brooks, W.; Swartz, J.; Figg, A.; Kubo, T. *Macromolecules*. **2016**, doi: 10.1021/acs.macromol.6b00181